ChemPubSoc Europe
DOI: 10.1002/open.201800034
Open Access ChemistryOPEN Reviews

Chromogenic and Fluorogenic Probes for the Detection of Illicit Drugs

Eva Garrido[+],[a] Luis Pla[+],[a] Beatriz Lozano-Torres,[a] Sameh El Sayed,[a, b] Ramón Martínez-Máñez,*[a, b, c] and Félix Sancenón[a, b, c]

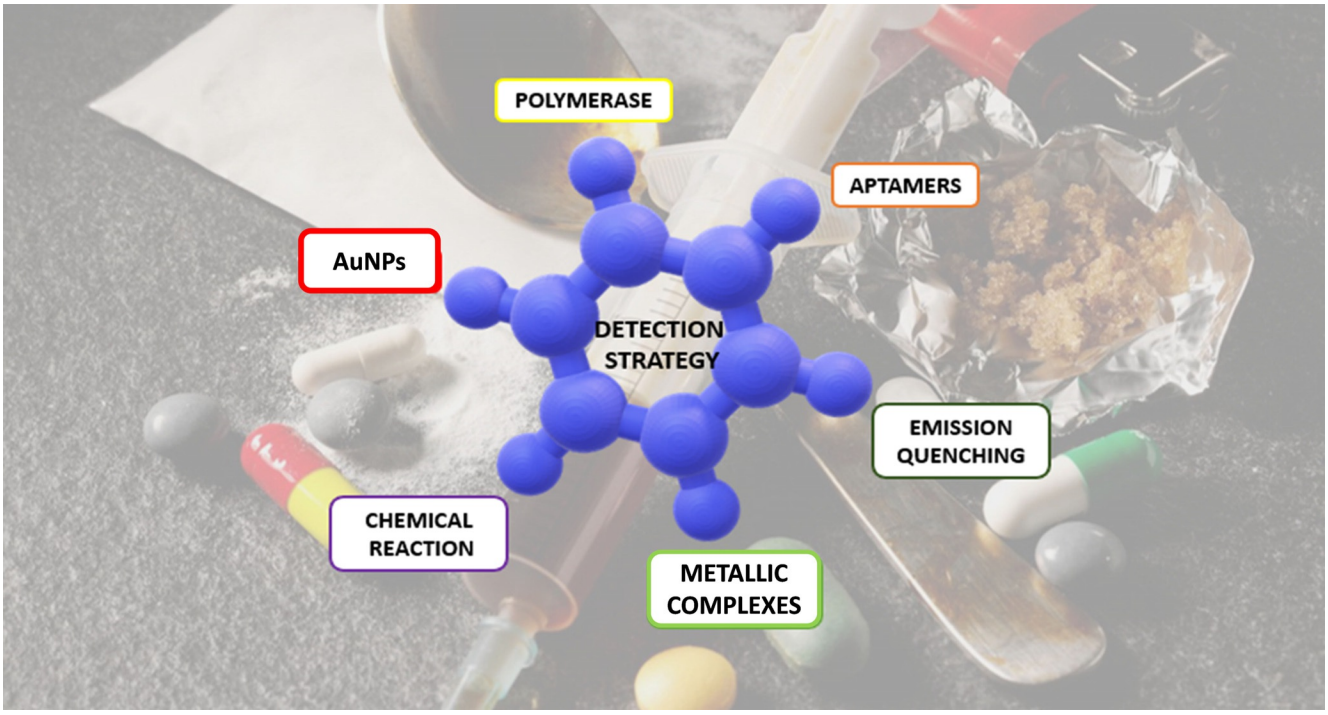

The consumption of illicit drugs has increased exponentially in recent years and has become a problem that worries both governments and international institutions. The rapid emergence of new compounds, their easy access, the low levels at which these substances are able to produce an effect, and their short time of permanence in the organism make it necessary to develop highly rapid, easy, sensitive, and selective methods for their detection. Currently, the most widely used methods for drug detection are based on techniques that require large measurement times, the use of sophisticated equipment, and qualified personnel. Chromo- and fluorogenic methods are an alternative to those classical procedures.

1. Introduction

The use of novel illicit drugs and the constant appearance of new psychoactive substances have rapidly grown in the last years, and reports of the availability and manufacture of such substances have increased.[1] Illicit drugs are those for which nonmedical use has been prohibited by international control treaties because they are believed to present unacceptable risks of addiction to users. According to the FDA, these compounds can also be defined as "drugs of abuse", substances that are used in a manner or amount inconsistent with the legitimate medical use.[2] The problematic use of these illicit drugs is associated with considerable mortality and morbidity. During the last 30 years, international control has been extended from plant-based drugs (e.g. heroin, cocaine, and cannabis) to synthetic drugs (e.g. amphetamines, 3,4-methylenedioxymethamphetamine, etc.) and pharmaceutical drugs (e.g. buprenorphine, methadone, benzodiazepines, etc.). Specifically, synthetic drugs are proliferating at an unprecedented rate and are posing significant public health challenges. The majority of these addictive substances, directly or indirectly, attack the brain's reward system, mainly serotonin and dopamine receptors, which regulate movement, emotion, motivation, and, above all, the feelings of pleasure and euphoria associated with the consumption of narcotics. Nowadays, amidst all illicit/abuse substances, cannabis is the most consumed drug worldwide with 183 million euro incautions, followed by amphetamines and derivatives (37 million euro), opioids (35 million euro), ecstasy (22 million euro), opiates (18 million euro), and cocaine (17 million euro). According to their pharmacologic behavior, drugs can be divided into depressants, stimulants, hallucinogenic, and opioids.

Because of their harmfulness to health, the ability to detect and quantify "drugs of abuse" in a fast, easy, and reliable way is crucial. The United Nations Office on Drugs and Crime (UNODC) established 28 million years of healthy life lost worldwide in 2015 because of premature death and disability caused by drug use.[3] Apart from the health problems generated by illicit drug consumption, UNODC exposes the existence of continue evolving organized crime/terrorism related with drug market. The European homologue, European Monitoring Centre for Drugs and Drug Addiction (EMCDDA), assumes there exists an important internet market dedicated to the sale of illicit substances protected by anonymization services.[4] Last annual informs of both the UNODCS and EMCDDA emphasized the necessity to control the production and distribution of new psychoactive substances (NPSs), as there are no assurances to the consumers of the compounds contained, and the need to reinforce the development of new detection systems with the aim to decrease and eliminate the abuse of traditional and synthetic emerging drugs.[5] The development of reliable methods for their detection and quantification is timely and urgently required.

Nowadays, illicit drug detection is performed mostly through chromatographic techniques, as can be seen by the large number of research articles published in this field, because of the excellent features of chromatographic techniques, which include great versatility, robustness, and sensibility.[6] Several electrochemical,[7] infrared,[8] Raman spectroscopy,[9] and magnetic resonance[1] methods also exist for the detection of several drugs, and these techniques show excellent results in terms of selectivity and sensibility. However, they present some shortcomings such as high cost, the use of trained personnel, tedious sample pretreatment, and so on. As an alternative to these traditional techniques, the design of molecular probes for the undemanding chromo- and fluorogenic detection of illicit drugs can be of importance. Both chromogenic and fluorogenic probes provide several advantages over other traditional analytical techniques, such as their chemical simplicity, ease of use, rapid response suitable for real-time on-site detection, easy detection to the naked eye, and so on.[10] Despite these remarkable features, the development of chromo- and fluorogenic sensors for the selective and sensitive detection of certain illicit drugs is still poorly explored. In this review, a thorough overview of chromogenic and fluorogenic sensing systems for the detection of most consumed drugs is provided.

[a] *E. Garrido,[+] L. Pla,[+] B. Lozano-Torres, Dr. S. El Sayed, Prof. R. Martínez-Máñez, Dr. F. Sancenón*
Instituto Interuniversitario de Investigación de Reconocimiento Molecular y Desarrollo Tecnológico (IDM), Universitat Politècnica de València
Universitat de València, Camí de Vera s/n, 46022 València (Spain)
E-mail: rmaez@qim.upv.es

[b] *Dr. S. El Sayed, Prof. R. Martínez-Máñez, Dr. F. Sancenón*
CIBER de Bioingeniería
Biomateriales y Nanomedicina (CIBER-BBN)

[c] *Prof. R. Martínez-Máñez, Dr. F. Sancenón*
Departmento de Química, Universitat Politècnica de València
Camí de Vera s/n, 46022 València (Spain)
E-mail: rmaez@qim.upv.es

[+] *These authors contributed equally to this work.*

The ORCID identification number(s) for the author(s) of this article can be found under: https://doi.org/10.1002/open.201800034.

The review is organized by the description of probes for different drugs classified according to their pharmacologic behavior, that is, depressants, stimulants, hallucinogenic, and opioids.

Table 1 contains a summary of the different strategies for the chromo- and fluorogenic detection of illicit drugs used in the examples described below.

Eva María Garrido graduated in chemistry from the University of Sevilla (US) in 2015 and received her Masters Degree (Masters in Food Technology and Industry) from the University of Seville (US) in 2016. She is a Ph.D. student at the Polytechnic University of Valencia (UPV), and her area of interest is the development of chemical sensors and probes based on the use of gated nanomaterials.

Luis Pla graduated in chemistry from the University of Valencia (UV) in 2013 and received his Masters Degree (Masters in Experimental and Industrial Organic Chemistry) from the University of Valencia (UV), University of Barcelona, Polytechnic University of Valencia, Cardenal Herrera University (CEU), and University of the Balearic Islands in 2014. He is a Ph.D. student at the Polytechnic University of Valencia (UPV), and his area of interest is the development of chemical sensors and probes based on the use of gated nanomaterials.

Beatriz Lozano-Torres graduated in chemistry from the Complutense University of Madrid (CUM) in 2013 and received her Masters Degree (Masters in Organic Chemistry) from the Complutense University of Madrid (CUM) in 2014. She is a Ph.D. student at the Polytechnic University of Valencia (UPV), and her main area of interest lies in developing chemical probes based on gated nanomaterials for biomedical applications.

Sameh El Sayed received his Masters Degree in chemistry from the Polytechnic University of Valencia (Spain) in 2012 and his Ph.D. degree from the same university in 2015 with Professor Ramón Martínez-Máñez. After a postdoctoral period at University of Pavia (Italy), he joined Centro de Investigación Biomédica en Red (CIBER) under a Juan de la Cierva postdoctoral fellowship for two years. His research areas of interest fall in the fields of chromo- and fluorogenic sensors and molecular probes for the detection of anions, cations, and neutral species, in addition to the development of nanomaterials for sensing and smart-delivery applications.

Ramon Martínez-Máñez was born in Valencia, Spain. He received his Ph.D. degree in Chemistry from the University of Valencia in 1986 and was a postdoctoral fellowship at Cambridge University, U.K. Presently, he is a full professor in the Department of Chemistry at the Polytechnic University of Valencia and is also the director of the IDM Research Institute at the Polytechnic University of Valencia and the Biomedical Research Networking center in Bioengineering, Biomaterials, and Nanomedicine (CIBER-BBN). He is the coauthor of more than 400 research publications and 20 patents. His current research interest involves designing gated hybrid materials for on-command delivery applications. He is also involved in developing new sensing methods for different chemicals of interest.

Felix Sancenón was born in 1968 in Manises, Valencia, Spain, and graduated in Chemistry in 1991. He received his Ph.D. degree in 2003. Afterwards, he worked with Professor L. Fabbrizzi at the Universitádi Pavia on the synthesis of chromogenic receptors for ion pairs. Then, he joined the Department of Chemistry at the Polytechnic University of Valencia with a Ramon y Cajal contract. He became a lecturer in 2006. He is the coauthor of more than 240 research publications. His current research interest comprise the use of hybrid materials for the development of sensors and for the design of gated materials.

Table 1. Summary of the different chromo- and fluorogenic methods for illicit drugs detection.[a]

Analyte	Recognition mechanism	Solvent	LOD [mg mL^{-1}]	Interferent	Ref.
DEPRESSANT DRUGS					
GBL	BODIPY fluorescent sensor	water and alcoholic drinks	3	–	[12]
GHB	BODIPY fluorescent sensor	beverages (alcoholic, nonalcoholic, colored, and colorless)	–	–	[14]
GHB	colorimetric sensor	water	–	GBL, 1,4-butanediol, propionic acid, butyric acid, and common salts	[15]
GHB	iridium(III) chemosensor	water, black tea, soda, orange juice, red wine, whisky, and milk	0.15	–	[16]
CPH	spectrophotometric method	water and pharmaceutical formulations	1.7×10^{-3}	–	[17]
ketamine hydrochloride	colorimetric test	water and pharmaceutical formulations	5	–	[18]
ketamine	colorimetric test	water	100	AMP, MAMP, MDMA, cocaine, EPH, scopolamine, caffeine, acetaminophen, ibuprofen, acetylsalicylic acid, starch, sugars, and $MgSO_4$	[20, 21]
drugs containing cyclic α-methylene carbonyl groups	fluorometric method	pharmaceutical preparations and biofluids	3×10^{-9} to 2×10^{-5}	–	[22]
dextromethorphan	spectrophotometric method	pharmaceuticals preparations	3.5×10^{-3}	–	[23]
morphine and codeine	AuNPs	human serum, urine samples, and pharmaceutical formulations	4.85×10^{-6} and 2.69×10^{-6}	cations, anions, ascorbic acid, glucose, urea, cysteine, glutamic acid, asparagine, leucine, valine, proline, phenylalanine, tramadol, AMP, and MAMP	[24]
STIMULANT DRUGS					
MA, EPH, and MeEPH	formation of colored product	urine	3.75×10^{-3}, 4.13×10^{-3}, and 4.48×10^{-3}	$CaCl_2$, NaCl, MgCl, $NaNO_3$, CH_3COONa, Al^{III}, Fe^{III}, Ni^{II}, Co^{II}, NH_4^+, urea, uric acid, creatinine, and hippuric acid	[26, 27]
AMP, MA, MDMA, and MDA	NPs	basic buffered aqueous	2–5	cocaine, cannabinol, cannabidiol, THC, scopolamine, EPH, and procaine	[28]
cocaine	biomimetic material (AuNPs)	absorbent pad	–	Benzoylecgonine, nicotine, cotinine, codeine, THC and MA	[29]
MA	Simon's reagent applied to mobile phone technology	application installed on a mobile phone	1.10×10^{-2} to 4.4×10^{-2}	–	[30, 31]
MDMA	bis-diarylurea-based probe	ecstasy tablets	2.45×10^{-5}	EPH, PEPH, AMP, MDA, and MDMA	[32]
MA	molecular recognition (thiophene heterocycles, fluorene, and polymer)	vapor	1.9×10^{-3} and 6.4×10^{-3}	–	[33]
MA	molecular recognition (perylene bisimide fluorophore, and two cholesterol subunits)	vapor	5.5×10^{-6}	amines, organic solvents, water, apple pomace	[34]
MDMA	NPs	water	0.95	cocaine, heroin, methadone, and morphine	[35]
MA	molecular recognition (amine-functionalized polyfluorene)	THF	2.5×10^{-5}	pethidine and EPH	[36]
MDMA	NPs	water	–	AMP, glucose, glycine, and sarcosine	[37]
AMPH, METH, MDMA; and DA	molecular recognition (macrocyclic)	H_2O/MeOH (7:3, *v/v*, pH 7.4)	7.4×10^{-6}, 1.3×10^{-6}, 8.0×10^{-6}, and 6.7×10^{-5}	–	[38]
MDMA and MDA	colorimetric reaction	sulfuric acid aqueous (75%, *w/v*)	0.19	–	[39, 40]
MA	NPs	toluene and vapor	–	*o*-toluidine, hexylamine, diethylamine, dibutylamine, allylamine, trimethylamine, and aniline	[41]
catecholamine	molecular recognition	water	–	biogenic amines, sugars, neurotransmitters, and amino acids	[42]
phenothiazine drugs	spectrophotometric method	sulfuric acid	–	–	[43]

Table 1. (Continued)

STIMULANT DRUGS					
PEA	UV	*n*-hexane	10^{-4}	phenylethanolamine	[44]
D- and L-α-phenylethylamines	fluorescence chiral sensors	MeCN	–	–	[45]
PEPH hydrochloride	spectrofluorometric method	PBS (pH 7.8)	0.5	additive or excipients present in the pharmaceuticals formulations	[46]
cocaine, MDMA/MDA, and heroine/morphine	spectral fluorescence signature (SFS) measurements	water	–	–	[47]
MA	aptasensor combined with AuNPs (colorimetric assay)	human urine	1.2×10^{-4}	pethidine, triazolam, barbital, morphine, ketamine, and diazepam	[49]
MA	aptasensor and oxidation reaction of a fluorophore	water	7.4×10^{-9}	ketamine, norketamine, morphine, methadone, cocaine, mephedrone, cathinone, methcathinone, 3-trifluromethylphenyl piperazine, 1-3-trifluromethylphenyl piperazine, 3,4-methylenedioxy pyrovalerona, MDA, MDMA, EDDP, and mCPP	[50]
cocaine	aptamer nanomachine (FRET process allowed or not depending on the analyte)	water	1.5×10^{-4}	–	[51]
cocaine	aptamer nanomachine and amplified aptamer nanomachine (quenching off/on process)	water	3.0×10^{-5} for normal and 3.5×10^{-17} for amplified process	–	[52]
cocaine	aptamer nanomachine (quenching off/on process)	water, saliva, serum, and urine	1.7×10^{-6}	–	[53]
cocaine	aptasensor combined with CQDs (quenching off/on process)	water	6.1×10^{-7}	benzoylecgonine and ecgonine methyl ester	[54]
cocaine	aptasensor combined with CQDs (quenching off/on process)	water	1.5×10^{-5}		[55]
cocaine	aptasensor combined with silica NPs and AuNPs (quenching off/on process)	water or serum	6.3×10^{-9} and 8.9×10^{-9}	chloramphenicol, propranolol, diazepam, and morphine	[56]
cocaine	fluorophore quenched by aptamer and recognition (quenching off/on process)	water, urine, and saliva	6.1×10^{-6}, 1.4×10^{-5}, and 1.5×10^{-5}	benzoylecgonine	[57]
cocaine	aptasensor combined with CQDs and NPs (quenching off/on process)	buffered solution	4.2×10^{-9}	benzoylecgonine, MA, 3-acetamidophenol, and codeine	[58]
cocaine	aptameric molecular gate (fluorogenic or SERS detection)	Tris solution (pH 7.5) and saliva	1.5×10^{-5}	morphine and heroine	[59,61]
cocaine	aptasensor (quenching off/on process)	buffered solution	3.0×10^{-5}	benzoylecgonine and ecgonine methyl ester	[62]
cocaine	aptasensor (quenching off/on process)	serum	3.0×10^{-4}	benzoylecgonine and ecgonine methyl ester	[63]
cocaine	aptasensor (molecular displacement of dye and increase in absorption band)	buffered solution	6.1×10^{-5}	benzoylecgonine and ecgonine methyl ester	[64]
cocaine	aptasensor (conformation changes after molecular recognition of analyte, high fluorescence anisotropy)	buffered solution	1.5×10^{-4}	theophylline, caffeine, BSA, IgG, arginine, phenylalanine, and aspartic acid	[65]
cocaine	aptasensor (conformation changes after addition of analyte in presence of CuNPs)	water	3.0×10^{-3}	ecgonine, pethidine, and methadone	[66]
cocaine	aptasensor combined with GO and AuNPs (quenching off/on process)	plasma and serum	3.0×10^{-3}	pethidine and methadone	[67,68]
cocaine	aptasensor combined with AuNPs (changes in absorption band due to aggregation of AuNPs)	water	6.1×10^{-5}	–	[69,70]
cocaine	aptasensor combined with AuNPs (changes in absorption band due to aggregation of AuNPs)	urine and serum	30.3	–	[71]

Table 1. (Continued)

STIMULANT DRUGS					
cocaine	aptasensor based on G-quadruplex/ruthenium complex interaction (decrease in fluorescence in presence of analyte)	serum	1.5×10^{-7}	caffeine, morphine, and theophylline	[72]
cocaine	aptasensor grafted onto optical fiber (quenching off/on process)	serum	5.0×10^{-6}	kanamycin, amikacin, and ibuprofen	[73]
cocaine	aptasensor combined with AuNPs (naked-eye detection system)	buffered solution	2.5×10^{-3}	ephedrine, codeine, ketamine, AMP, morphine, MA, benzoylecgonine, and ecgonine methyl ester	[74]
cocaine	aptasensor combined with AuNPs (changes in absorption band due to aggregation of AuNPs)	water	1.5×10^{-3}	–	[75]
cocaine	aptasensor combined with UCNPs and AuNPs (quenching off/on process)	saliva	3.0×10^{-6}	benzoylecgonine and ecgonine methyl ester	[76]
cocaine	aptasensor combined with GO and a fluorophore (quenching off/on process)	urine	5.8×10^{-5}	adenosine, caffeine, theophylline, and morphine hydrochloride	[77]
cocaine	aptasensor combined with CD and QDs (quenching on/off process)	serum	4.0×10^{-6}	MA, codeine, THC, nicotine, cotinine, and benzoylecgonine	[78]
cocaine and MA	aptasensor combined with Au@AgNPs (changes in absorption band due to aggregation of NPs)	buffered solution	1.5×10^{-7} for cocaine and 14.9 for MA	ketamine, norketamine, morphine, cathinone, methacathinone, 3-trifluoromethyphenylpiperazine, and MDA	[79]
cocaine	aptasensor based on G-quadruplex/iridium complex interaction (switch-on luminescence)	buffered solution	9.1×10^{-7}	ATP, adenosine, warfarin, and suramin	[80]
cocaine	aptasensor combined with MNPs	buffered solution	1.5×10^{-5}	ecgonine, pethidine, and methadone	[81]
cocaine	aptamer nanomachine combined with AgNPs (changes in fluorescence band due to aggregation of AgNPs)	serum	6.1×10^{-6}	ecgonine and benzoylecgonine	[82]
cocaine	aptasensor (conformation changes after molecular recognition of analyte, enhanced fluorescence intensity)	buffered solution	6.1×10^{-6}	benzoylecgonine and ecgonine methyl ester	[83]
HALLUCINOGENIC DRUGS					
LSD	fluorescence	water and NaOH	2.6×10^{-4} mg	mescaline, DOM, psilocin, psilocybin, bufotenin, ibogaine, and phencyclidine	[85]
OPIODS					
morphine, codeine, oxycodone, noroxycodone, thebaine, tramadol, and methadone	AuNPs	water	5 μmol L^{-1}	–	[87]
heroine, morphine, oxycodone, and their main metabolites	fluorescence	water and urine	7×10^{-8} for morphine and 8.25×10^{-5} and 2.78×10^{-6} for M3G and Nmor in water 2.75×10^{-5}, 9.72×10^{-4}, and 7.13×10^{-5} for morphine, M3G, and Nmor in urine	–	[88]

[a] LOD: limit of detection; GBL: γ-butyrolactone; GHB: γ-hydroxybutyric acid; CPH: chlorpromazine hydrochloride; AMP: amphetamine; MA: methamphetamine; MDMA: 3,4-methylenedioxymetamphetamine; MDA: 3,4-methylenedioxyamphetamine; EPH: ephedrine; MeEPH: methylephedrine; THC: tetrahydrocannabinol; PEPH: pseudoephedrine; DOM: 2,5-dimethoxy-4-methylamphetamine; AMPH: (+)-amphetamine sulfate; METH: (+)-methamphetamine hydrochloride; DA: dopamine; PEA: 2-phenylethylamine; EDDP: 2-ethylidene-1,5-dimethyl-3,3-diphenylpyrrolidine; mCPP: *meta*-chlorophenylpiperazine; IgG: immunoglobulin G; BSA: bovine serum albumin.

2. Depressant Drugs

Depressant drugs slow down the nervous system and brain activity and thus have a sedating effect.[11] Most depressants affect one of the brain's neurotransmitters, that is, γ-aminobutyric acid (GABA), which upon activation produces a sense of calm and relaxation. GABA is the chief inhibitory neurotransmitter in the mammalian central nervous system (CNS), and its principal role is to reduce neuronal excitability. Depressant drugs have the particularity that often leads to "drug tolerance", which makes the organism ask for higher doses until dependence or overdose arises. Coma, respiratory diseases, and death are the potential consequences of their continuous consumption. Depressant drugs comprise barbiturates, benzodiazepines, alcohol, and γ-hydroxybutyrate.

In 2013, Chang and co-workers reported boron–dipyrromethene (BODIPY) fluorescent sensor **3** for γ-butyrolactone (GBL) detection in water and in different alcoholic drinks (Figure 1).[12] GBL is a prodrug of γ-hydroxybutyric acid (GHB),

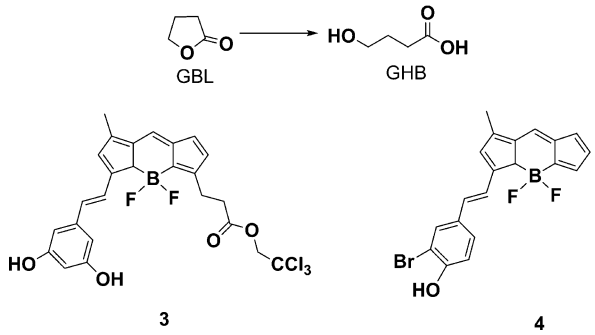

Figure 1. Structures of probes **3** and **4** for the detection of GBL (**1**) and GHB (**2**), respectively.

and its relevance is due to the strong regulation to which GBH is subject, but this is not applicable to GBL. GBL overdose causes irrational behavior, severe sickness, coma, and death.[13] Sensor **3** shows a marked absorption band centered at $\lambda = 569$ nm in water. Besides, upon excitation at $\lambda = 569$ nm, a small emission band at $\lambda = 582$ nm (with a low quantum yield of 0.05) is observed. The addition of GBL to an aqueous solution of **3** induces an emission enhancement at $\lambda = 582$ nm ($\approx$10-fold). A limit of detection for GBL by using **3** is reported to be 3 mg mL^{-1}. The off–on emission response is related with the hydrophobic character of the probe. The authors indicate that probe **3** forms nonemissive aggregates in water that are progressively broken upon coordination with GBL with a subsequent enhancement in emission. In addition, probe **3** can be used to detect GBL in drink samples after a simple extraction process. The presence of GBL is simply assessed by irradiation with a green laser pointer; this induces the appearance of orange fluorescence, which is not observed in samples without the drug.

The same authors also report on the preparation of BODIPY probe **4** (Figure 1) for the fluorogenic detection of GHB.[14] Ethanol/water (1:1, *v*/*v*) solutions of **4** show an absorption band at $\lambda = 557$ nm and emission at $\lambda = 574$ nm. The addition of GHB induces moderate emission quenching (2.2-fold in the presence of 10 mg mL^{-1} of the drug) of the band at $\lambda = 574$ nm. This behavior can be ascribed to the formation of a hydrogen bond between the phenolic hydrogen atom of the probe and the carboxylate moiety of the drug. As a consequence of the coordination, a photoinduced electron-transfer (PET) process is activated, which induces the observed emission quenching. Moreover, the authors demonstrate that probe **4** can be used to detect GHB easily in several beverages (alcoholics, nonalcoholics, colored, and colorless). For this purpose, **4** is dissolved in DMSO and then mixed with the beverages spiked with known amounts of GHB (1:1, *v*/*v*, final solution). Irradiation of the prepared samples with a hand-held lamp ($\lambda = 365$ nm) allows differences in the fluorescence intensities of GHB-free and GHB-spiked beverages to be observed clearly by the naked eye.

Garcia and co-workers have developed a colorimetric sensor array for the detection of GHB.[15] The array is composed of three columns and six rows. The first column has six tricyclic dyes (methylene blue, thionine, oxonine, pyronine, acridine orange, and proflavine), the second column is formed by the same dyes complexed with cucurbit[7]ril (CB[7]), and the third column contains the dyes complexed with cucurbit[8]ril (CB[8]). The addition of GBH (in the 0.1–10^{-5} M range) to the sensor array induces remarkable color changes in some plates due to the dethreading of CB[7] and CB[8] complexes with the dyes after coordination of the macrocycles with the drug. The colors obtained are ascribed to the different stability constants for the dye–CB complexes and to the ability of GBH to disrupt the formed supramolecular ensembles. Moreover, the chromogenic response of the array to GHB is quite selective, and other possible interferents, such as GBL, 1,4-butanediol, propionic acid, butyric acid, and common salts present in water, are unable to induce color changes.

Ma and co-workers outline the synthesis of a long-lived iridium(III) chemosensor, the luminescence emission of which at $\lambda = 570$ nm is quenched in the presence of GHB (Figure 2).[16] Due to its long-lived luminescence, time-resolved emission spectroscopy (TRES) allows the detection of GBH. A quenching effect of 30% luminescence emission is observed 10 s after the addition of a low concentration of GBH (0.15 mg mL^{-1}) to a solution of the complex. This quenching is clearly seen by the naked eye under UV illumination and is not pH dependent. Real samples of water, black tea, soda, orange juice, red wine,

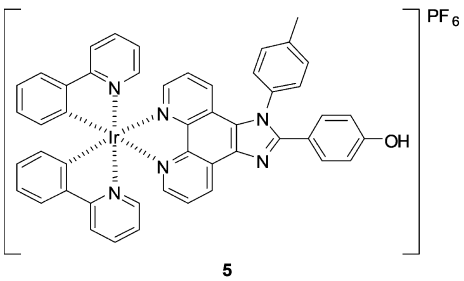

Figure 2. Chemical structure of iridium probe **5**.

whisky, and milk previously spiked with GHB have been evaluated, which assures the suitability of this procedure for GHB drug detection over a wide range of real-life beverages.

Al-Kaffiji and co-workers have developed a spectrophotometric method for the optical detection of chlorpromazine hydrochloride (CPH). CPH pertains to the family of drugs commonly known as neuroleptic tranquilizers (used as sedatives, antihistamines, and anesthetics) but nowadays is commonly mixed with narcotic drugs.[17] The method is based on the reaction of *p*-aminoacetanilide (**7**) with CPH in the presence of an oxidizing agent (i.e. ferric chloride hexahydrate). This reaction yields an intense violet product (see structure **8** in Scheme 1) with an intense absorption band at $\lambda = 590$ nm. Probe **7** has successfully been applied to the determination of CPH in aqueous solutions and pharmaceutical formulations with high accuracy and shows a linear range between 4 and 32 ppm with a limit of detection of about 1.7 ppm.

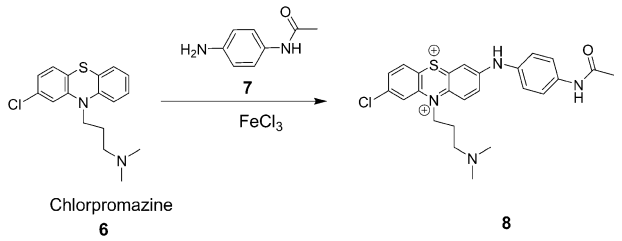

Scheme 1. Oxidation reaction with *p*-aminocetanilide (**7**) and ferric chloride for the detection of chlorpromazine drug **6**.

Morris has developed a colorimetric test for ketamine hydrochloride on the basis of a typical cocaine detection assay by using $Co(SCN)_2$.[18] Ketamine is a medication mainly used for starting and maintaining anesthesia, but it is also a drug for recreational purposes. Unregulated use has side effects such as high blood pressure, abnormal heart rhythms, vomiting, double and tunnel vision, anaphylaxis, airway obstruction, and dependence.[19] The test consists of the basification of the samples (with sodium hydroxide) followed by the addition of $Co(SCN)_2$. This two-step procedure results in the formation of a lavender to purple precipitate in the presence of ketamine, whereas a blue to green precipitate is obtained in the absence of ketamine. Sensibility as high as 5 mg mL^{-1} can be achieved, which is good enough for the detection of this drug in commercial products for medical applications (contents ranging from 50 to 100 mg mL^{-1}). Selectivity studies show that other controlled substances and related chemicals yield a negative response.

Herráez-Hernández and co-workers follow a similar reaction for the colorimetric sensing of ketamine by immobilizing different amounts of the $Co(SCN)_2$ reagent onto a polydimethylsiloxane (PDMS) matrix.[20] For the preparation of the materials, the authors disperse $Co(SCN)_2$ in an aqueous solution containing tetraethylorthosilicate (TEOS) and expose the resulting dispersion to PDMS to embed $Co(SCN)_2$ in the polymer matrix.[21] Once the sensing material is prepared, pure ketamine detection can be performed by immersing the sensor in 0.1 M NaOH solutions of the drug. In the presence of ketamine, a purple precipitate on the surface of the matrix polymer is formed. However, after a few minutes, this precipitate disappears, and the solid changes from brown to purple because of the diffusion of ketamine inside the polymer and the formation of a complex between $Co(SCN)_2$ and the drug. The best response is observed for a solid containing 0.3% $Co(SCN)_2$ at $\lambda = 625$ nm. A limit of detection of 100 μg mL^{-1} for ketamine is reported. Besides, no interference is observed if the sensing material is exposed to amphetamine, methamphetamine, 3,4-methylenedioxymethamphetamine (MDMA), cocaine, ephedrine, scopolamine, caffeine, acetaminophen, ibuprofen, acetylsalicylic acid, starch, saccharose, glucose, lactose, and magnesium sulfate. The material has been tested in real samples with fine results.

Elokely and co-workers describe the design of a new fluorometric method for the detection of drugs containing cyclic α-methylene carbonyl groups in pharmaceuticals, preparations, and biofluids by using *N*-methylnicotinamide chloride (NMNCl) as a fluorogenic reagent (Scheme 2).[22] In basic media, *N*-methylnicotinamide chloride forms neutral and highly reactive α-carbinol compound **12**, which reacts with drugs containing cyclic α-methylene carbonyl groups (such as **9**, **10**, and **11**) to yield fluorescent derivative **15**. The test is quite sensitive with limits of detection in the 0.003–20 ng mL^{-1} range. The authors also demonstrate the possible use of *N*-methylnicotinamide for the detection of drugs **9**, **10**, and **11** in plasma samples with nearly the same limits of detection obtained upon using water.

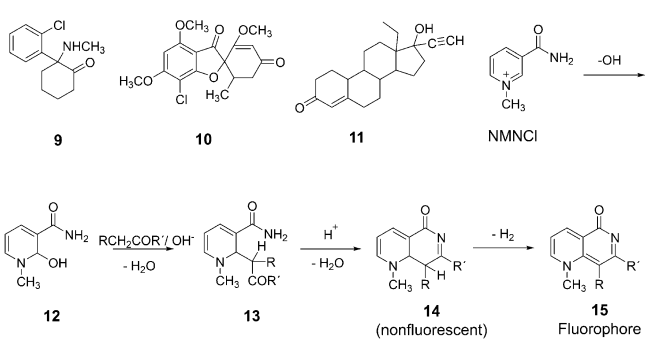

Scheme 2. Chemical structures of drugs **9–11** containing cyclic α-methylene carbonyl groups, and synthetic pathway for the preparation of fluorophore **15**.

Elmosallamy and Amin have developed a new spectrophotometric method for the detection of dextromethorphan (**16**) (Figure 3) in pharmaceutical preparations.[23] The spectrophotometric protocol involves the reaction between dextromethorphan hydrobromide with eriochrome black T (**17**) in acetate buffer (pH 2.8), which results in the formation of an ion-pair complex with an absorption band at $\lambda = 520$ nm. This method for the detection of **16** is lineal in the $7.37–73.7 \times 10^{-5}$ M range with a limit of detection of 1.29×10^{-5} M.

Mohseni and Bahram outline the use of melamine-coated gold nanoparticles (AuNPs) for the detection of morphine and codeine in human serum, urine samples, and pharmaceutical formulations.[24] The presence of melamine molecules in the

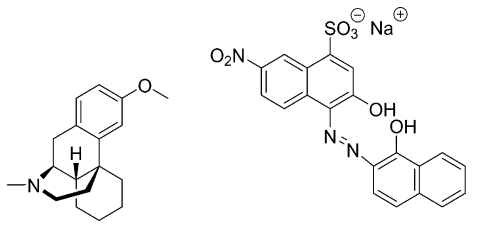

16 17

Figure 3. Chemical structures of the drug dextromethorphan (**16**) and eriochrome black T (**17**).

outer sphere of the AuNPs prevents aggregation, and aqueous solutions of the nanoparticles present as a wine-red color (absorption band centered at $\lambda = 675$ nm). In the presence of morphine and codeine, a marked color change to blue is observed (absorbance band at $\lambda = 690$ nm) due to the aggregation of the AuNPs induced by the formation of hydrogen bonds between melamine and the drugs. The proposed method exhibits lineal ranges of 0.07 to 3 μM for morphine and 0.03 to 0.8 μM for codeine with limits of detections of 17 and 9 nM, respectively. Interference studies show that cations, anions, ascorbic acid, glucose, urea, cysteine, glutamic acid, asparagine, leucine, valine, proline, phenylalanine, tramadol, amphetamine, and methamphetamine are unable to induce color modulations. Besides, melamine-coated AuNPs have also been used for the detection of morphine and codeine in biological fluids and pharmaceutical formulations with fine results.

The probes described in this section are based on different chemical reactions and the formation of complexes with depressant drugs. Also, the analyte-induced aggregation of AuNPs has been used to detect morphine and codeine. High selectivity and low detection limits are achieved with most of the probes exposed above, and thus, they are good alternatives for traditional chromatographic methods. Naked-eye detection, short analysis times, and no need for overqualified personnel for their daily use are some of the advantages of these sensing probes. Besides, some probes have been tested in real human body fluids, and thus, some of these reported examples could have potential applications for the development of realistic systems for the detection of depressant drugs.

3. Stimulant Drugs

Stimulant drugs accelerate the activity of the central nervous system. If high doses are taken, elevated blood-pressure levels and increased heart and respiration rates may ensue, with the potential risk for cardiovascular failure; however, these drugs can also make consumers feel angry and/or paranoid.[25]

Normally, these drugs inhibit the reuptake of serotonin, norepinephrine, and dopamine, which results in greater concentrations of these three neurotransmitters in the brain, and this leads to multiple effects on the state of mind of the individual user. There are a number of stimulant drugs, including those that are legal and prescribed by doctors and those that are considered illegal. In the group of legal drugs, caffeine and nicotine are the most common. On the other hand, cocaine, crack, amphetamine, and their derivatives are found among illegal stimulant drugs.

Sakai and Ohno describe a procedure for the sensitive and selective detection of methamphetamine, ephedrine, and methylephedrine in urine (Scheme 3).[26,27] The method consists in the extraction of basified urine containing the drugs with 1,2-dichloroethane. Then, the organic phase, which contains

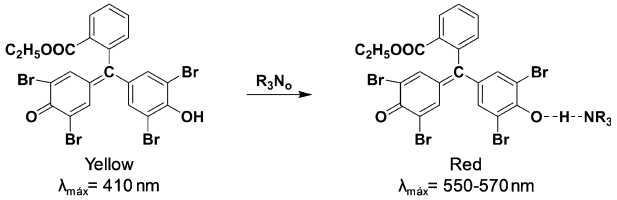

18 19

Scheme 3. Tetrabromophenolphthalein ethyl ester **18** transformation into red-colored product **19** in the presence of methamphetamine, ephedrine, and methylephedrine in urine.

the drugs, is added to a 1,2-dichloroethane solution of tetrabromophenolphthalein ethyl ester (**18**). After a few minutes, colored product **19** is formed. The absorption maxima are found at $\lambda = 570$ nm for methamphetamine, $\lambda = 555$ nm for ephedrine, and $\lambda = 550$ nm for methylephedrine. The procedure described presents high selectivity, and calcium chloride, sodium chloride, magnesium chloride, sodium nitrate, sodium acetate, Al^{III}, Fe^{III}, Ni^{II}, Co^{II}, ammonium ions, urea, uric acid, creatinine, and hippuric acid are all unable to induce any chromogenic response. In addition, the limits of detection are 3.75 μg mL^{-1} for methamphetamine, 4.13 μg mL^{-1} for ephedrine, and 4.48 μg mL^{-1} for methylephedrine.

Herráez-Hernández and co-workers embed 1,2-naphthoquinone-4-sulfonate **20** (Figure 4) into polydimethylsiloxane/tetraethylorthosilicate/silicon dioxide nanoparticles and use this mixture to identify amphetamine (AMP), methamphetamine (MAMP), 3,4-methylenedioxymethamphetamine (MDMA), and 3,4-methylenedioxyamphetamine (MDA) chromogenically.[28] Basic buffered aqueous suspensions of the nanoparticles show a light yellow color due to the presence of a broad absorption band at around $\lambda = 460$ nm. Upon the addition of amphetamines, clear color changes to orange (for MAMP and MDMA, which are secondary amines) or gray-brown (for AMP and MDA, which are primary amines) are observed. Limits of detection in the 0.002–0.005 g mL^{-1} range are found. The prepared sensing material displays better selectivity for amphetamines than for other drugs such as cocaine, cannabinol, cannabidiol, tetrahydrocannabinol (THC), scopolamine, ephedrine, and pro-

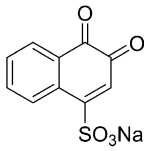

20

Figure 4. Chemical structure of 1,2-napthoquinone-4-sulfonate (**20**) used for the detection of amphetamine-based drugs.

caine. The only two drugs that interfere with amphetamine detection are ephedrine and prococaine. The application of this sensing system to real ecstasy samples allows the percentage of amphetamine contained in the pills to be calculated. Comparing these results with those obtained by LC methods, no significant differences are found.

Yagci and co-workers delineate a strategy involving the use of a noncompetitive assay format by using a biomimetic material, poly(phenylene)β-cyclodextrin poly(ethylene glycol) (PPP-CD-g-PEG), to recognize cocaine due to the affinity of β-CD toward this drug (Figure 5).[29] The authors prepare test strips

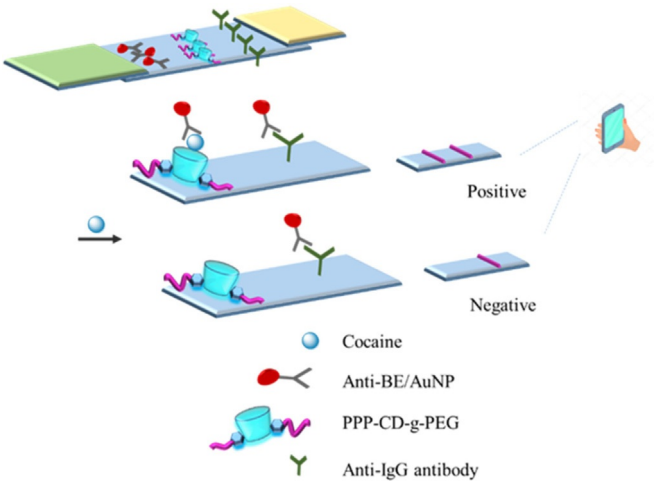

Figure 5. Schematic representation of a test stripe functionalized with PPP-CD-g-PEG and Anti-IgG antibodies for the detection of cocaine.

composed of a polyvinyl chloride (PVC) backing card, the sample pad, the conjugate release pad, a nitrocellulose membrane, and an absorbent pad. In the absorbent pad, there is a conjugated pad [containing absorbed antibenzoylecgonine antibody/AuNPs (Anti-BE/AuNPs)], a control line (containing absorbed Anti-IgG antibody), and a test line (containing absorbed PPP-CD-g-PEG). Upon applying a liquid sample without cocaine to the sample pad and upon reaching the conjugate pad, the Anti-BE/AuNPs migrate forward together with the liquid sample to give a red negative line. If cocaine is present in the sample, cocaine molecules interact with the β-CD residues in the test line and another red line appears in the test zone as a result of the attachment of the Anti-BE/AuNPs to cocaine. The test results can also be analyzed by using a mobile phone application by photographing the strips and evaluating the color group and color percentage in the image. A good linear trend in the 0.01–1.0 $\mu g\,mL^{-1}$ range is observed. Moreover, the authors find that the sensor is selective for cocaine in the presence of benzoylecgonine, nicotine, cotinine, codeine, tetrahydrocannabinol, and methamphetamine. Finally, the authors demonstrate the validity of the test stripes by determining cocaine in synthetic saliva with nearly the same accuracy as that achieved by using chromatographic methods.

Simon's reagent (a mixture of sodium nitroprusside, sodium carbonate, and acetaldehyde) is a chromogenic test used for the detection of alkaloids (containing secondary amines). The amine moiety of the alkaloids reacts with acetaldehyde to yield an enamine, which subsequently reacts with sodium nitroprusside to generate an immonium salt. Finally, this is hydrolyzed to a bright cobalt-blue product (known as the Simon–Awe complex) that allows for the identification of drugs containing secondary amines. Chooduma and co-workers use this reagent to sense methamphetamine by using mobile phone technology.[30] In their study, the samples (containing methamphetamine) are kept in an opaque black corrugated box and are treated with Simon's reagent; the intensity of the colored product inside the microtube is then detected by using the ColorAssist app (FTLapps,Inc.) for an iPhone 4.0 in the flash-off mode. The authors relate the RGB values obtained to the concentration of methamphetamine and then compare the data with the gas chromatography data. The authors note that the correlation between both sets of data, in terms of methamphetamine concentration, is remarkable. Besides, one year later, the same authors report the entrapment of Simon's reagent into a sol–gel matrix and include it in the corrugated box.[31] For sample analysis, the solid sensor is pierced and methamphetamine is put inside to allow the reaction between the analyte and the reagent. The samples are then directly analyzed by using the same app by studying the RGB values.

Torroba and co-workers describe the synthesis of new bis-diarylurea-based probe **21** (Figure 6) for the detection of MDMA

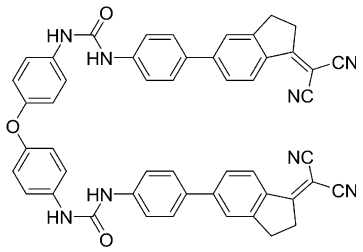

21

Figure 6. Chemical structure of bis-diarylurea-based probe **21** for MDMA detection.

from ecstasy tablets.[32] DMSO solutions of probe **21** show a weak emission band centered at $\lambda = 517$ nm upon excitation at $\lambda = 288$ nm. The addition of aqueous solutions of ephedrine, pseudoephedrine, amphetamine, 3,4-methylenedioxyamphetamine, and 3,4-methylenedioxymethamphetamine induces a marked emission enhancement at $\lambda = 517$ nm due to the formation of a 1:1 stoichiometry complex of a charge-transfer nature. In spite of the fact that the fluorogenic response of probe **21** toward selected drugs is unselective, principal component analysis (PCA) score plots allow their discrimination. Besides, MDMA has been detected in a simulated tablet of ecstasy. No interference is observed in the presence of excipients (e.g. sucrose, chalk, or caffeine) in ecstasy tablets.

Cheng and co-workers give details on the preparation of molecular probe **22** containing thiophene heterocycles and a fluorene moiety (Figure 7) and also polymer **23** containing the

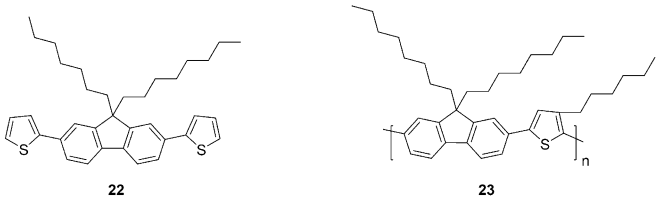

Figure 7. Structures of thiophene-containing fluorene derivatives **22** and **23** for MA detection.

same functional groups for methamphetamine (MA) vapor detection.[33] Films of the molecular probe and the polymer are obtained by spin coating. The prepared films are weakly fluorescent, but in the presence of MA, a marked emission enhancement is observed for both sensing materials. The weak emission of the films is ascribed to a heavy-atom effect from the sulfur atom of the thiophene to the fluorene fluorophore. In the presence of MA, the reaction of its amino groups with the thiophene rings of compounds **22** and **23** induces a marked reduction in the heavy-atom effect with a subsequent emission enhancement. Limits of detection of 1.9 and 6.4 ppm for MA by using films containing **22** and **23** have been measured. Besides, exposure of the films to vapors of propylamine, aniline, or toluidine induces negligible changes in the emission intensity.

Following a similar concept, Fang and co-workers design a perylene bisamide-containing film for methamphetamine vapor detection.[34] Molecular probe **24** (Figure 8), containing a perylene bisimide fluorophore and two cholesterol subunits, is able to form self-assembly fluorescent films on a glass surface. A broad emission band at $\lambda = 678$ nm is observed for the film that is absent in the probe alone. This emission can be ascribed to the formation of fluorescent aggregates of the probe within the film (through π–π interactions). This emission band of the film is markedly quenched in the presence of methamphetamine vapor with a limit of detection of 5.5 ppb. Vapors of aniline, xylidine, *o*-toluidine, and 1,4-diaminobenzene also induce moderate emission quenching. Moreover, the authors demonstrate that the film can be easily reused by purging with cold air.

Lozano-Torres and co-workers recount the preparation of mesoporous silica nanoparticles (MSNs) capped with pseudorotaxanes for the selective and sensitive fluorogenic detection of

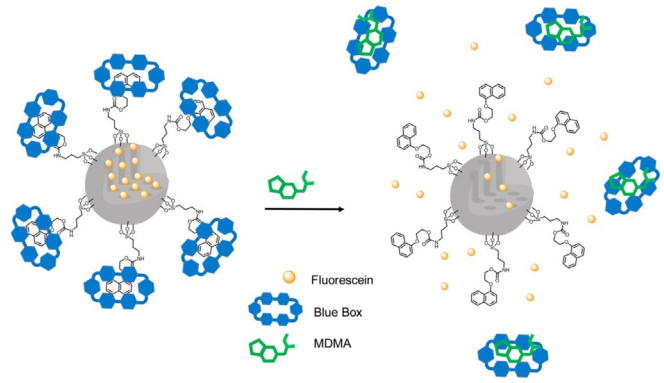

Scheme 4. Schematic representation of MDMA detection by using silica nanoparticles and the [CBPQT][PF_6]$_4$ macrocycle.

MDMA in water (Scheme 4).[35] In a first step, the external surface of the MSNs is functionalized with a naphthalene derivative, and this is followed by the encapsulation of fluorescein inside the porous network of the inorganic scaffold. In a second step, the loaded MSNs are capped upon the addition of the cyclobis(paraquat-*p*-phenylene) hexafluorophosphate ([CBPQT][PF_6]$_4$) macrocycle, which forms inclusion complexes with 1-naphtol subunits attached onto the external surface of the nanoparticles. Aqueous suspensions of the nanoparticles at pH 7.0 show negligible fluorescein release, whereas in the presence of MDMA a marked emission band at $\lambda = 520$ nm ($\lambda_{ex} = 495$ nm) in the solution is found. The observed emission band can be ascribed to the release of fluorescein from the nanoparticles due to the preferential coordination of MDMA with the $CBPQT^{4+}$ macrocycle, which results in pore opening and cargo delivery. Besides, the prepared material is selective to MDMA, and other common drugs (e.g. cocaine, heroin, methadone, and morphine) are unable to induce the release of fluorescein. A limit of detection of 4.9 mM for MDMA in water has been determined.

He and co-workers detail the synthesis and characterization of an amine-functionalized polyfluorene for the detection of methamphetamine.[36] THF solutions of the prepared polyfluorene show two broad emission bands at $\lambda = 417$ and 440 nm (upon excitation at $\lambda = 388$ nm) due to the fluorene core. The addition of methamphetamine induces a marked quenching of the emission bands (80% upon the addition of 40 μM drug), which can be ascribed to an aggregation process of the poly-

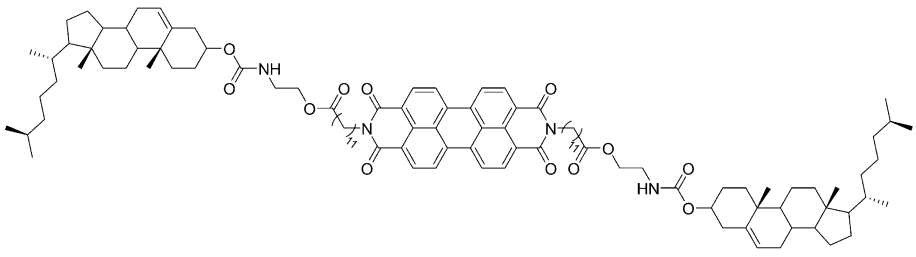

24

Figure 8. Perylene bisamide based probe **24** for MA detection.

mer. From the emission titration profiles, a limit of detection of 25 ng mL^{-1} of methamphetamine hydrochloride is noted. Other drugs such as pethidine and ephedrine also induce marked quenching of the emission.

Prodi, Dalcanale, and co-workers report the preparation of silica nanoparticles with pyrene derivative **25** inserted and with a hydrophilic external surface due to the presence of a poly(ethylene glycol) shell for MDMA detection in water (Figure 9).[37] Aqueous suspensions of the prepared nanoparticles present the typical monomer/excimer emission spectrum of the pyrene fluorophore with bands at about $\lambda = 395$ and 475 nm. Upon the incorporation of cavitand **25** into the hydrophobic compartment of the nanoparticles, both pyrene units are in close spatial proximity, which allows the formation of an excimer (band centered at $\lambda = 475$ nm). The addition of increasing quantities of MDMA induces progressive and marked quenching of only the excimer band. The authors ascribe this fact to the inclusion of the amine moiety of MDMA into the cavitand, which induces spatial separation of both pyrene fluorophores and disrupts initial excimer **26**. The addition of 3-fluoromethamphetamine (FMA) also induces excimer emission quenching but to a lesser extent than that observed for MDMA. Amphetamine, glucose, glycine, and sarcosine are unable to induce any emission change.

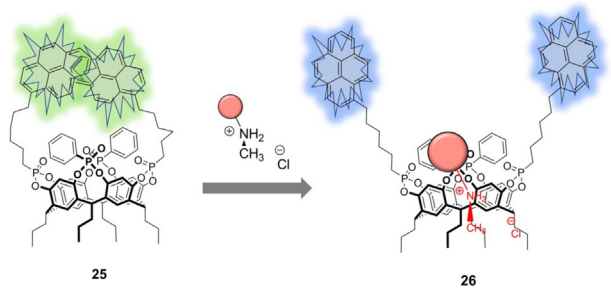

Figure 9. Schematic representation of MDMA detection by interaction with pyrene derivative **25**.

García-España and co-workers report the synthesis of macrocyclic probes **27** and **28** (Figure 10) containing fluorene and naphthalene fluorophores and their sensing behaviors towards amphetamine sulfate (AMPH), methamphetamine hydrochloride (METH), 3,4-methylenedioxymethamphetamine hydrochloride (MDMA), and dopamine (DA).[38] A water/methanol (7:3, *v/v*, pH 7.4) solution of probe **27** shows typical fluorene emission bands at $\lambda = 377$, 396, and 416 nm. The addition of AMPH, METH, MDMA, and DA to a solution of **27** induces a marked emission enhancement that is nearly of the same order for the four drugs and ascribed to the formation of 1:1 adducts. In contrast, more selective behavior is found with naphthalene-bearing probe **28**. In this case, a water/methanol (7:3, *v/v*, pH 7.4) solution of **28** shows the typical naphthalene emission band that is enhanced only upon the addition of MDMA and DA.

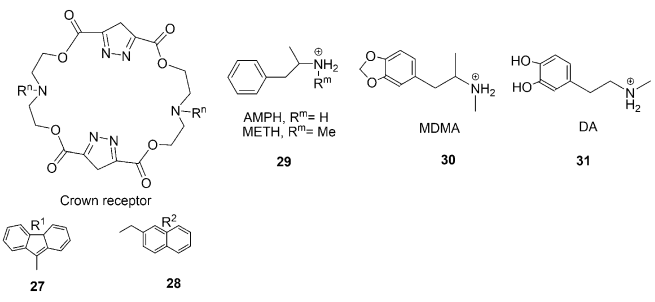

Figure 10. Chemical structures of macrocyclic probes **27** and **28** for the detection of drugs **29**, **30**, and **31**.

Ishii and co-workers present an optimized version of a previously published method[39] for the detection of MDMA, MDA, and related drugs that consists in a rapid colorimetric reaction with chromotropic acid (CTA) in 75% (*w/v*) aqueous sulfuric acid at room temperature (Scheme 5).[40] In this protocol, formaldehyde (**33**) is generated by treating MDMA with sulfuric acid. Then, formaldehyde induces the coupling of two CTA molecules to yield red-violet product **34** that can be examined visually or by measuring its absorbance at $\lambda = 570$ nm. The band at $\lambda = 570$ nm gradually increases with an increase in the drug concentration. The optimal concentration of CTA and the optimal reaction time are 1.0 mM and 30 min, respectively, whereas the drug concentration should not be greater than 100 μM to avoid nonspecific color development. Finally, seized tablets containing well-known concentrations of both MDMA and MDA have been processed and analyzed by using the proposed methodology.

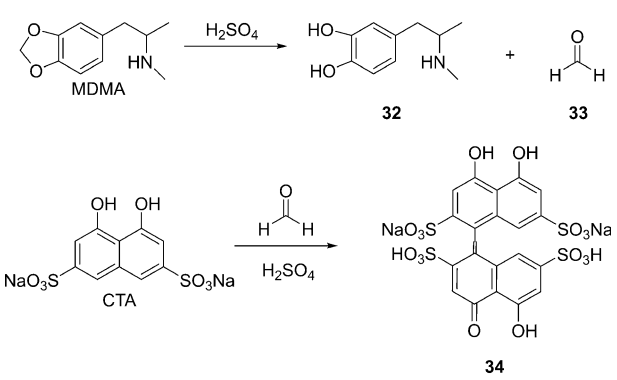

Scheme 5. MDMA detection through the generation of formaldehyde. Formed formaldehyde reacts with CTA to yield red-violet product **34**.

Haghgoo and Rouhani describe the synthesis of 1,8-naphtalimide–thiophene derivative **35**, which is further attached to silica nanoparticles to give **35**@SiO_2.[41] Toluene solutions of **35** present a broad emission band centered at $\lambda = 435$ nm, which shifts to $\lambda = 473.5$ nm if grafted onto silica nanoparticles. The addition of methamphetamine to a solution of probe **35** (Figure 11) or to a suspension of the nanoparticles (using toluene in both cases) induces marked emission enhancements (7.3 and 15.4-fold for free **35** and **35**@SiO_2, respectively). These emission enhancements can be ascribed to inhibition of the heavy-atom effect (from the thiophene ring) upon coordination of the probes with methamphetamine. In contrast, negligi-

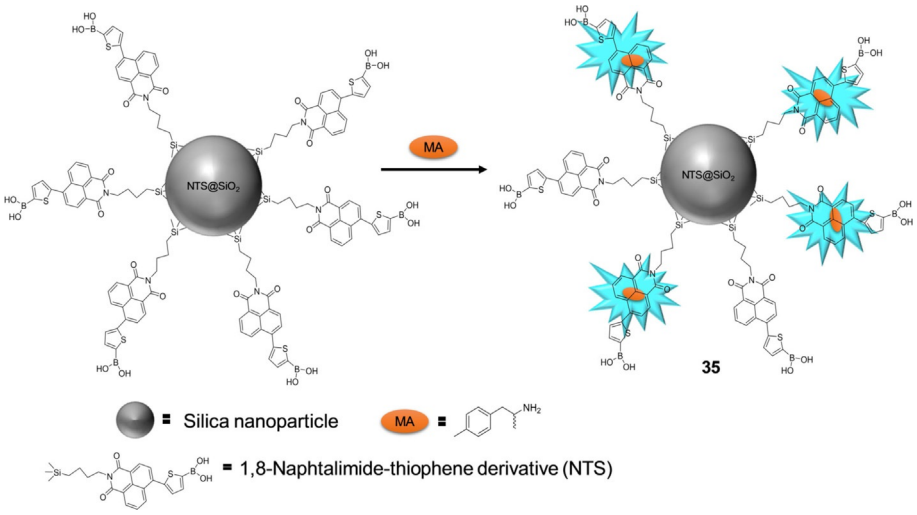

Figure 11. MA detection process with functionalized nanoparticles **35**@SiO_2.

ble fluorescence changes are observed for other amines such as *o*-toluidine, hexylamine, diethylamine, dibutylamine, allylamine, and trimethylamine, whereas slight quenching is found for aniline. Furthermore, methamphetamine vapor sensitivity has successfully been evaluated by exposing analyte-saturated vapors (6.7 $\mu mol\,L^{-1}$ to 0.27 $mmol\,L^{-1}$ concentration) over **35**@SiO_2 on glass, which shows reversibility after vapor removal. Finally, the proposed probe has been validated with HPLC, and there is satisfactory agreement between the results obtained with both methods.

Maue and Schrader outline the design and synthesis of a new family of catecholamine probes (i.e. compounds **36**–**38**) combining bisphosphonate recognition moieties (for amino alcohols) and boronic acid groups (for the recognition of catechols) in one chemical structure.[42] The addition of alizarine red-S to aqueous solutions of the three probes induces a marked color change from deep red (free dye with an absorbance band at $\lambda \approx 520$ nm) to orange (band centered at $\lambda =$ 460 nm) due to the formation of 1:1 complexes (Figure 12). In the presence of noradrenaline, a marked decrease in the band at $\lambda = 460$ nm is observed together with an increase in the absorbance at $\lambda = 520$ nm (color change from orange to deep red). These changes in color can be ascribed to preferential coordination of noradrenaline with the probes that displace alizarine red-S from the sensing ensemble to the solution. Several potential interferents have been examined, and no positive response for simple biogenic amines (creatinine), sugars (e.g. glucosamine, glucose, fructose, saccharose), neurotransmitters (e.g. γ-aminobutyric acid, serotonin, acetylcholine), and amino acids (e.g. serine, phenylalanine, alanine, histidine, lysine, tryptophan, glycine) is observed.

Basavaiah and co-workers design a spectrophotometric method for the determination of six phenothiazine drugs (i.e. chlorpromazine hydrochloride, promethazine hydrochloride, trifluoromazine hydrochloride, trifluoperazine hydrochloride, thioproperazine mesylate, and prochlorperazine mesylate) in pharmaceutical preparations.[43] This method is based on the

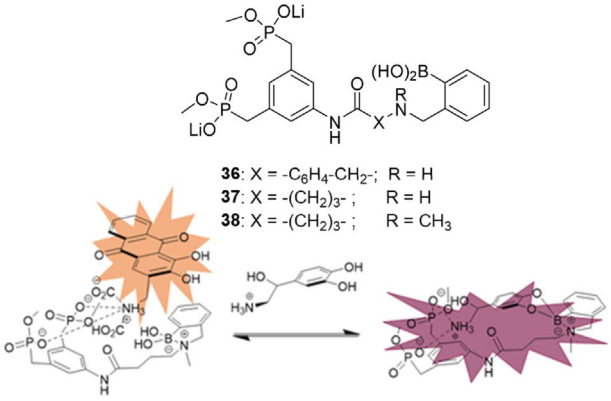

Figure 12. Chemical structures of catecholamine probes **36**–**38** and recognition mechanism. Alizarine red-S is displaced in the presence of noradrenaline due to higher affinity with the probe.

oxidation of the drugs in sulfuric acid medium by a known excess amount of chloramine-T. Then, the excess amount of chloramine-T reacts with 4-*N*-methylaminophenol in the presence of an aromatic amine to produce a purple-red product with an absorption maximum at $\lambda = 520$ nm.

Inwang and Mosnaim report the development of an efficient and specific extraction procedure for the UV spectrophotometric detection of 2-phenylethylamine (PEA) through reaction with ceric sulfate ($CeSO_4$) to form a fluorescent probe.[44] Samples are treated with $CeSO_4$ and HCl in *n*-hexane, and this is followed by filtration and extraction of the aqueous layer. This procedure has also been evaluated for biological samples, in addition to real human, cat, and rabbit organs as well as urine. A linear relationship is found between the concentration of PEA and the UV absorbance at $\lambda = 287$ nm, with a limit of detection of 0.1 $\mu g\,mL^{-1}$.

Wang and co-workers discuss the development of two fluorescence chiral sensors for the enantiomeric recognition of D- and L-α-phenylethylamines (Figure 13).[45] The author prepared

39 40

Figure 13. Chemical structures of fluorescent dimeric and oligomeric probes **39** and **40** for L-α-phenylethylamines.

dimeric and oligomeric binaphthol derivatives **39** and **40**, respectively, for detection through a host–guest interaction between **39** or **40** with the chiral amines. It is suspected that the chiral amines interact with the host through π–π interactions between the naphthyl moieties and the amino phenyl group. These interactions produce changes in the emission intensity of the probes depending on the concentration of the guest molecule. As most amines do not have chromophores, the typical emission at $\lambda = 410$ nm for the naphthalene ring of the host structures can be used to follow changes in the fluorescence intensity. With the addition of different concentrations of the chiral guest phenylethylamines, the fluorescence quantum yield of the solutions can be measured, and fluorescence emission reversion behavior is observed. The fluorescence responses of these two developed chiral sensors are influenced by the concentration of the target chiral amines. The recognition can be confirmed by ^{1}H NMR spectroscopy measurements.

El-Didamony and Gouda report on the development of a spectrofluorometric method for the detection of pseudoephedrine (**41**) in commercial pharmaceutical formulations in pure and dosage forms through its derivatization with 4-chloro-7-nitrobenzofurazan (**42**) (Scheme 6).[46] Compound **42** itself is non-emissive but upon reaction with thiols or amines, it forms highly fluorescent product **43**. In phosphate-buffered saline (PBS, pH 7.8), **41** reacts with **42** to yield a strongly emissive derivative with a band at $\lambda = 532$ nm. The authors optimize several parameters such as pH, buffer, concentration, solvent, and temperature finally to propose a method that can measure concentrations of **41** down to 0.5 mg mL^{-1} with good accuracy and precision.

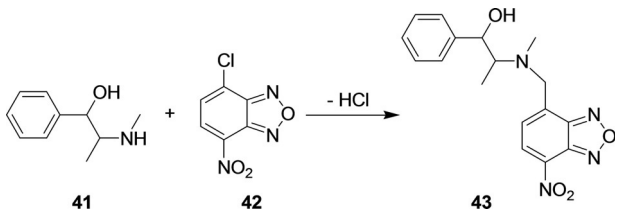

41 42 43

Scheme 6. Detection of **41** by derivatization with 4-cloro-7-nitrobenzofurazan (**42**). The reaction results in the formation of fluorescent adduct **4**.

Poryvkina and co-workers validate a new procedure for the detection of several common street drugs such as cocaine, MDMA/MDA, and heroine/morphine on the basis of spectral fluorescence signature (SFS) measurements and artificial neuron networks (ANNs).[47] SFS analyses generate a two-dimensional spectra matrix for which the intensity depends on the excitation/emission wavelengths and the concentration of the analyte. For cocaine detection, the fluorescence emission intensity at $\lambda = 315$ nm can be evaluated ($\lambda_{ex} = 235$ and 273 nm) with an enhancement and quenching in the presence of cocaine salt. On the other hand, the MDMA fluorescence emission intensity at $\lambda = 320$ nm ($\lambda_{ex} = 235$ and 285 nm) is enhanced if the drug is present. To differentiate MDMA from MDA, the samples can be treated with *o*-phthalaldehyde-*N*-acetylcysteine (OPA-NEC), which forms selectively an isoindole complex with MDA with a maximum emission at $\lambda = 425$ nm ($\lambda_{ex} = 335$ nm). On the other hand, heroin analysis is based on the detection of morphine in the sample due to the great similarity of their corresponding structures. The fluorescence of heroin in water is not strong enough to confirm the presence of heroin in multicomponent samples, but the presence of morphine can be detected because of its high quantum yield of fluorescence. For this purpose, samples are treated with hydrochloric acid to convert morphine into the morphine salt. Growth of the fluorescence signal is observed at $\lambda = 345$ nm ($\lambda_{ex} = 285$ nm) after treatment. The designed protocol shows excellent selectivity and limits of detection. Besides, 98.7% of samples are correctly identified, assuring the robustness of the method. Due to the great amount of data generated, the use of ANN as a tool for pattern recognition of SFS is required, which includes a learning step and posterior validation.

One of the most extensive strategies for the fluorogenic and chromogenic detection of drugs is based on aptasensors, which are a class of biosensor systems based on the use of DNA or RNA aptamers as recognition sites. Aptamers can recognize selectively certain target molecules through the formation of a specific three-dimensional site obtained due to nucleotide chain folding.[48] Aptasensors usually show very high sensitivity, specificity, and reproducibility against a wide variety of targets.

As an alternative to traditional chemosensors for methamphetamine (MA) detection, Shi and co-workers present a simple colorimetric assay for the sensitive and visual detection of this drug in both aqueous solution and human urine.[49] The proposed strategy comprises the advantages of using a selective methamphetamine aptamer (as the recognition element) and unmodified easy-to-prepare AuNPs (as an indicator). In a first step, citrate-coated AuNPs are prepared, and then, the cocaine aptamer is adsorbed onto the external surface of the nanoparticles. An aqueous solution of the aptamer-coated AuNPs shows the characteristic plasmon absorption band at $\lambda = 525$ nm (red color), which is indicative of the presence of nonaggregated individual nanoparticles. The addition of increasing amounts of methamphetamine induces the progressive appearance of an absorption band centered at $\lambda = 660$ nm with a subsequent color change from red to blue. This change in color can be ascribed to coordination of methamphetamine

with the coating aptamer, which induces aggregation of the AuNPs (Figure 14). Using a calibration curve, the reported aptasensor is able to detect methamphetamine in aqueous solutions at concentrations ranging from 2 to 10 μM with a limit of detection of 0.82 μM. The aptasensor is also able to detect methamphetamine in urine with recoveries ranging from 96.0 to 107.0% and with high selectivity against potential competing alkaloids such as pethidine, triazolam, barbital, morphine, ketamine, and diazepam.

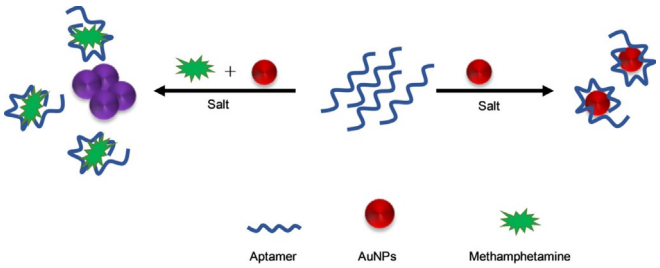

Figure 14. Schematic representation of MA colorimetric detection consisting in the preferential interaction of the aptamer with the drug rather than with AuNPs.

Li et al. outline the construction of a colorimetric methamphetamine probe consisting of a G-quadruplex–hemin DNAzyme molecular beacon, a drug aptamer, and a colorimetric substrate (Figure 15).[50] In the presence of methamphetamine, the DNAzyme dissociates because of strong interactions between the drug and its aptamer, and this results in the formation of a G-quadruplex–hemin complex with peroxidase activity that catalyzes the oxidation reaction of 2,2′-azinobis(3-ethylbenzothiozoline)-6-sulfonic acid to yield a light-green derivative with an absorbance band at $\lambda = 415$ nm. The proposed aptamer-based probe shows excellent linearity with the methamphetamine concentration and a limit of detection of 0.5 nM. The selectivity with 15 other illicit drugs or metabolites (i.e. ketamine, norketamine, morphine, methadone, cocaine, mephedrone, cathinone, methcathinone, 3-trifluromethylphenyl piperazine, 1-(3-trifluromethylphenyl)piperazine, 3,4-methylenedioxypyrovalerona, MDA, MDMA, 2-ethylidene-1,5-dimethyl-3,3-diphenylpyrrolidine, and *meta*-chlorophenylpiperazine) has been evaluated, yet none of them show a significant UV/Vis response.

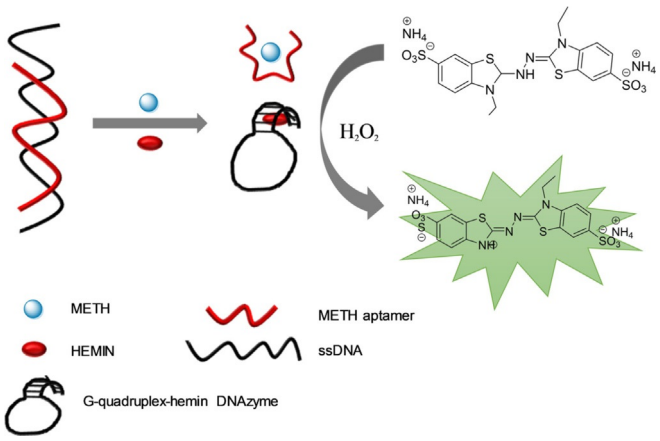

Figure 15. Colorimetric methamphetamine aptasensor based on the peroxidase activity of the formed G-quadruplex–hemin complex resulting in the oxidation of 2,2′-azinobis(3-ethylbenzothiozoline)-6-sulfonic acid to a light-green-colored derivative. ssDNA = single-stranded DNA.

Willner and co-workers report the design of an aptamer-based nanomachine for the fluorogenic detection of cocaine.[51] The nanomachine contains three regions: 1) a cocaine aptamer; 2) a nicking site for endonuclease (Nt.BbvCI); 3) a transduction region (Figure 16). Initially, the aptamer recognizes the cocaine molecule, and then, in the presence of polymerase and 2′-deoxynucleosidetriphosphates (dNPTs), the complementary strand is synthesized (see Figure 16b). Then, region 2 is nicked by Nt.BbvCI endonuclease, and this is followed by a cyclic process by which the complementary region is repeatedly polymerized with the aid of the polymerase enzyme. The released transduction region (see Figure 16d) hybridizes with its complementary strand, which separates the two fluorophores (i.e. carboxyfluorescein and 5-carboxytetramethylrhodamine) and forbids the fluorescence resonance energy transfer (FRET) process to which they were submitted. Finally, a limit of detection of 5×10^{-6} M for cocaine can be achieved.

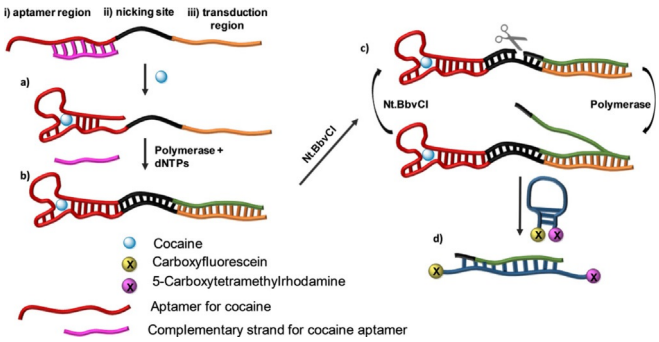

Figure 16. Fluorogenic aptasensor for the detection of cocaine: a) cocaine recognition, b) complementary strand synthesis, c) nicking with Nt.Bbv.CI followed by polymerization, and d) hybridization of the synthesized strand with fluorescent conjugated hairpin structure that avoids the FRET process and allows carboxyfluorescein emission.

The same authors have also created an amplified aptamer sensor for cocaine (Figure 17).[52] The developed system is formed by three domains: 1) a domain that corresponds to the cocaine aptamer, which is blocked by the complementary strand; 2) a domain containing a nicking strand; 3) the transduction region. In presence of cocaine, the system begins the replication and nicking processes; this releases domain 3, which is complementary to the strand containing a fluorophore and a quencher (off state). Then, the DNAzyme cleaves the fluorophore/quencher to yield the fluorophore-labeled strand (separated from the quencher) that provides the readout signal for the analysis of cocaine (on state). The limit of detection for cocaine is 0.1 μM. Finally, a method for amplified cocaine detection has been developed by the coupling of a second replication/nicking system that includes an autono-

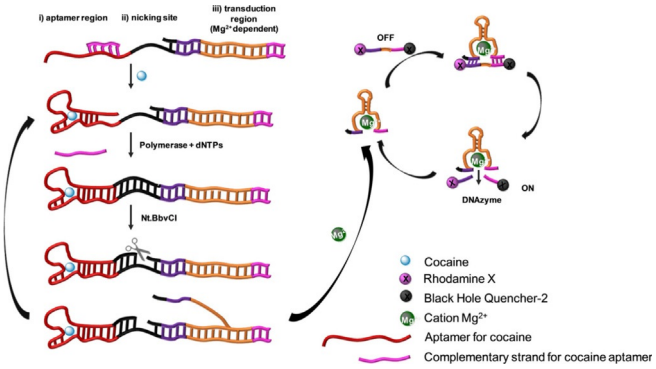

Figure 17. Schematic representation of the cocaine aptasensors.

mous self-replication process. The limit of detection for the amplified system is 1×10^{-18} M; this is roughly 10^4-fold more sensitive than other DNA-sensing platforms.

Wang and co-workers validate the use of a fluorescence label-free aptasensor for detecting cocaine in complex biofluids.[53] The system consists of an aptamer and two fluorophores, 2-amino-5,6,7-trimethyl-1,8-naphthyridine (ATMND) and SYBR Green I (SGI), which serve as a signal reporter and a built-in reference, respectively. Both fluorophores interact strongly with the aptamer, and as a consequence, their fluorescence is quenched. However, if cocaine is added, an enhancement in the fluorescence emission of ATMND is observed. This emission enhancement can be ascribed to the fact that ATMND coordinates with the binding cavity of the aptamer and is displaced in the presence of cocaine. The authors report a limit of detection of 56 nM. The system has been tested in biofluids (e.g. saliva, serum, and urine) with fine results.

Huang and co-workers detail the design of a new system based on a strand-displacement polymerization reaction by using aptamer recognition for the detection of cocaine (Figure 18).[54] The system consists of a hairpin probe labeled with Cy5 (acceptor fluorophore) on its 3′-end and containing the cocaine aptamer sequence, a primer derivatized on its 5′-end with carboxy fluorescein (a donor fluorophore), and a polymerase (which induces DNA sequence synthesis). If cocaine is present, the hairpin probe recognizes the drug and the polymerase induces DNA synthesis; this results in proximity between the donor and acceptor fluorophore, which leads

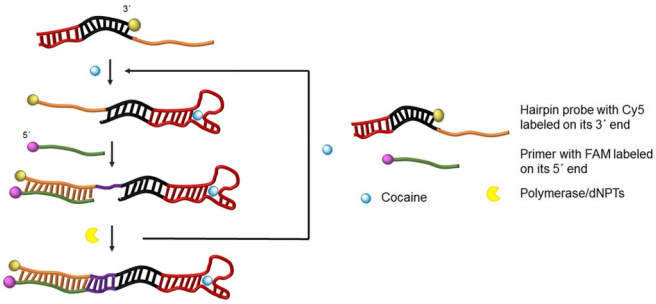

Figure 18. Schematic representation of a cocaine aptasensor based on the actuation of polymerase and interaction of two fluorophores in the presence of the drug.

to a fluorescence enhancement. The limit of detection for cocaine is 20 nM. Finally, the authors also evaluate the systems in the presence of benzoylecgonine and ecgonine methyl ester. Neither of the tested interferents induce emission changes.

Johnson and co-workers discuss the development of an aptameric cocaine sensor based on FRET between quantum dots (QDs) and the fluorophore Cy5 (Figure 19).[55] For this purpose,

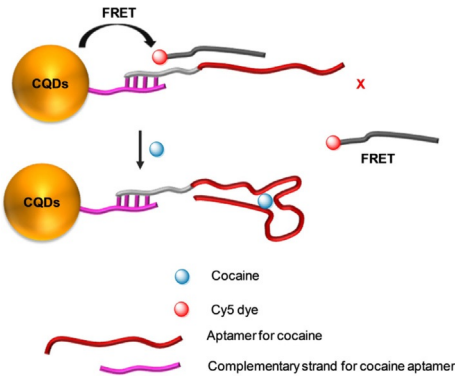

Figure 19. Cocaine aptasensor operating scheme. In the presence of cocaine, the aptamer changes to a hairpin conformation and avoids the FRET process and suppresses Cy5 emission. CQDs = carbon quantum dots.

QDs coated with streptavidin are functionalized with the single-stranded DNA sequence 5′-TCA CAG ATG AGT-biotin-3′. Then, the cocaine aptamer is sandwiched between this oligomer and 5′-GTC TCC CGA GAT-Cy5-3′. Upon excitation of the QDs at $\lambda = 605$ nm in an aqueous suspension of the sensor, the typical emission band of the Cy5 fluorophore at $\lambda \approx 675$ nm appears due to the presence of a FRET process between the nanoparticles and the fluorophore. However, in the presence of cocaine, the random-coil aptamer changes to a hairpin conformation, which releases the Cy5 fluorophore brand with subsequent suppression of the FRET process. As a consequence, the emission of Cy5 is progressively quenched depending on the amount of cocaine added. The limit of detection for cocaine is 0.5 μM, as determined by a titration profile. Besides, the authors modify the probe to obtain an emission enhancement as output. For this purpose, they include a Cy5 quencher into the probe structure. The surface of the QDs is functionalized with 5′-Cy5-TCA CAG ATG AGT-biotin-3′. The cocaine aptamer is again sandwiched between this oligomer and 5′-GTC TCC CGA GAT-Iowa Black RQ-3′ containing a quencher of Cy5. The presence of the quencher inhibits the FRET process between the QDs and Cy5. In the presence of cocaine, the quencher oligomer is released due to a change in the aptamer to the hairpin conformation and the FRET process occurs with a subsequent turn-on response. The limit of detection for cocaine is 0.5 μM, as determined by a titration profile.

Abnous and co-workers merge two different types of nanoparticles to construct an aptasensor for the fluorogenic detection of cocaine.[56] The authors first prepared silica nanoparticles coated with streptavidin and functionalized with 5′-fluorescein-ATT GAA GGA TTT ATC CTT GTC TCC CTA TGC TTC AAT-biotin-3′ (complementary sequence to that of the cocaine

aptamer). On the other hand, they also prepare AuNPs functionalized with the 5′-CCA TAG GGA GAC AAG GAT AAA TCC TTC AAT GAA GTG GGT CTC CC-thiol-3′ sequence containing the cocaine aptamer. Upon mixing both nanoparticles, the complementary strands hybridize, and the emission of fluorescein is quenched because the fluorophore is in close proximity to the AuNPs. The addition of cocaine induces dehybridization of the double-stranded DNA fragment due to drug–aptamer coordination. This process detaches both types of nanoparticles, and as a consequence, fluorescein emission is restored. Besides, the limits of detection of cocaine in water (209 pM) and serum (293 pM) have been determined. The authors find that chloramphenicol, propranolol, and diazepam are unable to induce any emission enhancement, whereas morphine yields the same response as cocaine.

Xiao et al. report a label-free aptamer–fluorophore ensemble to detect cocaine.[57] The authors observe that the typical aptamer used to recognize cocaine is able to complex the fluorophore 2-amino-5,6,7-trimethyl-1,8-naphthyridine (**44**) (Figure 20). Due to complexation, fluorescence of **44** is quenched. However, in the presence of cocaine, the complex between the aptamer and the fluorophore is disrupted, and an emission enhancement is observed. The authors note a limit of detection of 200 nM in water. Besides, the sensing ensemble allows the selective detection of cocaine in the presence of its metabolite benzoylecgonine. In urine and saliva, the aptasensor presents limits of detection of 460 and 520 nM, respectively.

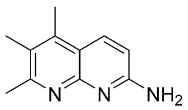

44

Figure 20. Structure of 2-amino-5,6,7-trimethyl-1,8-naphthyridine (**44**).

Coskunol et al. create an aptamer-folding-based sensing device for cocaine detection.[58] Poly-L-lysine-coated microwells are used as inorganic supports and QDs functionalized with carboxylic acid groups are grafted onto the surface by using *N*-hydroxysuccinimide (NHS)/1-ethyl-3-(3-dimethylaminopropyl)carbodiimide (EDC). On the other hand, AuNPs functionalized with the cocaine aptamer sequence 5′-NH_2-C6-AGA CAA GGA AAA TCC TTC AAT GAA GTG GGT CG-C3-SH-3′ are anchored to the QDs also by using NHS/EDC. In the absence of cocaine, strong fluorescence from the QDs is observed, whereas in the presence of the drug, this emission is quenched (Figure 21). This emission quenching can be ascribed to coordination of the aptamer to cocaine, which brings the QDs close to the AuNPs with subsequent fluorescence deactivation. The same response is observed for benzoylecgonine. The limits of detection for cocaine and its metabolite are 0.138 nM and 1.66 μM, respectively. The aptasystem is selective for cocaine and benzoylecgonine in the presence of methamphetamine, 3-acetamidophenol, and codeine. Finally, upon analyzing synthetic urine samples containing cocaine and benzoylecgonine with the sensing material and comparing the results with those obtained by traditional HPLC methods, no significant differences are found.

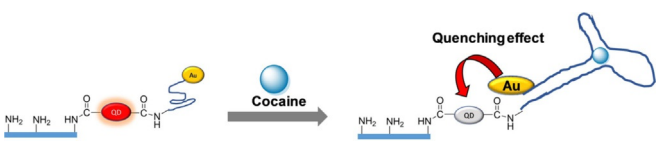

Figure 21. Schematic illustration for cocaine detection by using an aptamer and AuNPs.

Martínez-Máñez and co-workers implement "molecular gates" onto nanoporous anodic alumina (NAA) to prepare a sensing material for cocaine detection (Figure 22).[59] The NAA support, obtained according to reported procedures,[60] is loaded with rhodamine B and functionalized with (3-isocyanatopropyl)triethoxysilane. Then, the amino-terminal DNA sequence NH_2-$(CH_2)_6$-5′-AAA AAA CCC CCC-3′ is covalently linked to the surface by the formation of urea bonds. In a final step, the pores are capped with the 5′-TTT TGG GGG GGG GAG ACA AGG AAA ATC CTT CAA TGA AGT GGG TCT CCA GGG GGG TTT T-3′ sequence, which specifically hybridizes with the short DNA fragment attached to the external surface of NAA and contains the cocaine aptamer. If the sensing material is immersed in Tris solution (pH 7.5) without cocaine, negligible dye release is observed. However, in the presence of the drug, marked rhodamine B delivery is found (reaching 100% after 50 min). Using a calibration curve obtained upon adding increasing amounts of cocaine, a limit of detection of 5.0×10^{-7} M is calculated. Besides, the material presents good selectivity for cocaine, and no response is observed by exposing it to other drugs such as morphine and heroine. Finally, the sensor has been validated in saliva. The same research group has developed a homologous nanostructured system for the detection of cocaine by surface-enhanced Raman spectroscopy (SERS).[61]

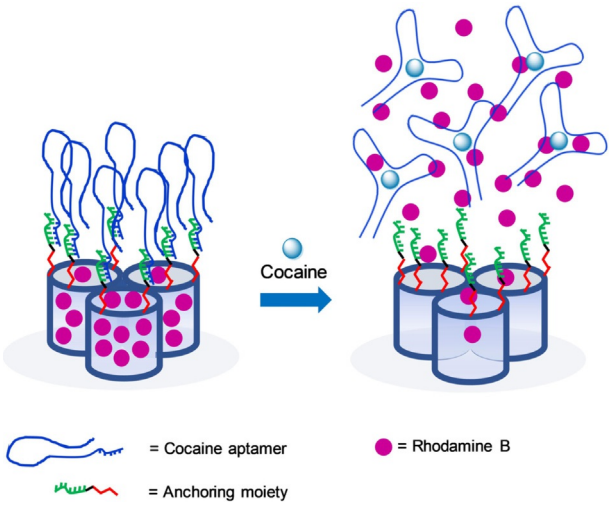

Figure 22. Schematic representation for cocaine detection by using silica nanoparticles with a fluorescent dye encapsulated and an aptamer as molecular gates.

Landry and co-workers outline the development of a cocaine sensor based on the assembly of fluorophore-labeled heterodimeric aptamers in the presence of the analyte.[62] The authors prepare two oligonucleotides containing the cocaine aptamer

sequence. One of the oligonucleotides is labeled with a 5′-carboxyfluorescein fluorophore, whereas the other is functionalized with the well-known fluorescence quencher dabcyl at the 3′-position. In the presence of cocaine in a buffered solution and with optimal oligonucleotide chain concentration, heterodimerization of both aptameric sequences results in fluorescein emission quenching at $\lambda = 518$ nm (Figure 23). This sensor has

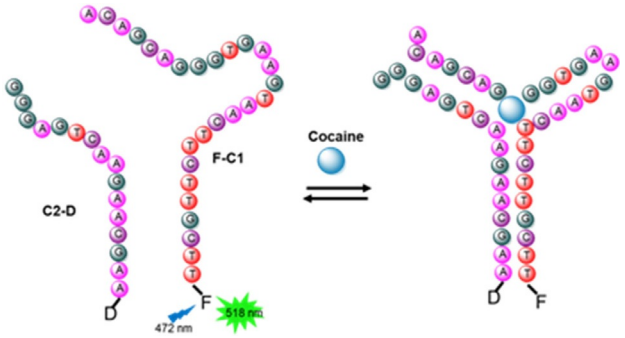

Figure 23. Conformational change in the aptamer in the presence of cocaine and subsequent fluorescent emission quenching.

a limit of detection of 1 μM and has excellent selectivity, as no quenching effect is observed in the presence of the cocaine metabolites benzoylecgonine and ecgonine methyl ester.

The same authors have also engineered a new method for the detection of cocaine in serum by using a deoxyribonucleotide-based aptamer (Figure 24).[63] The proposed method consists of an aptamer that is designed taking into account that binding with cocaine induces a marked change in its secondary structure and, as a consequence, in the emission of a grafted fluorophore. The authors construct a double-labeled aptamer with 5′-fluorescein as the fluorophore and 3′-dabcyl as the quencher. In the absence of cocaine, both the fluorescein and quencher are far away, and excitation of the fluorophore results in its emission at $\lambda = 518$ nm. However, in the presence of cocaine, the aptamer changes its conformation upon coordination with the drug, and thus, the fluorophore

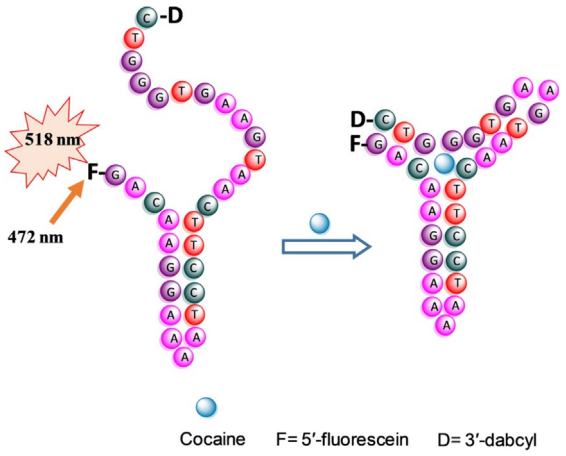

Figure 24. Conformational change in the aptamer in the presence of cocaine and subsequent fluorescent emission quenching.

and quencher come into close proximity. As a consequence, the emission of fluorescein is quenched. The aptamer allows the detection of cocaine in the 10 μM to 2.5 mM range. Finally, the authors demonstrate that the sensor is highly selective for cocaine and is useful for the screening of cocaine hydrolases.

In 2002, Landry and Stojanovic developed another cocaine sensor that consists in the displacement of a cyanine dye from the hydrophobic pocket generated by anticocaine aptamer MNS-4.1 upon binding with the drug (Figure 25).[64] The au-

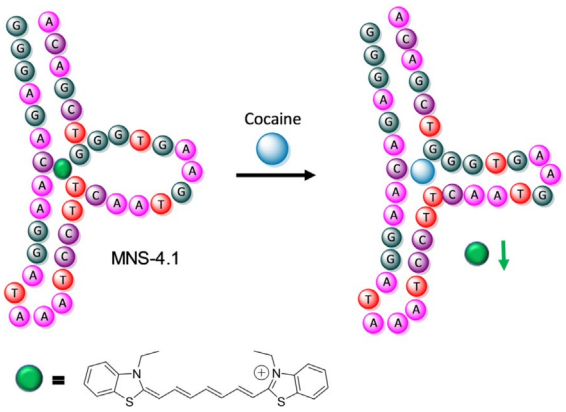

Figure 25. Displacement of cyanine dye from the hydrophobic pocket generated by the anticocaine aptamer if the cocaine drug is present.

thors screen 35 different dyes to find one that displays both significant attenuation of absorbance and a change in the ratio of two relative maxima. Thus, the authors select diethylthiotricarbocyanide dye and mix it with the aptamer MNS-4.1 in a buffered media. Then, increasing concentrations (2 to 600 μM) of cocaine are added, and a decrease in the absorption at $\lambda = 760$ nm is observed (whereas the absorption band at $\lambda = 670$ nm remains unaltered). Negligible changes in the visible spectra are found upon adding the cocaine metabolites benzoylecgonine and ecgonine methyl ester (up to 2 mM). Finally, marked color changes (from colorless to blue) are observed upon using higher dye and aptamer concentrations (40 and 20 μM, respectively) in the presence of 500 μM cocaine.

Recently, Liu and Zhao presented an aptasensor labeled on a specific position at one G base with the tetramethylrhodamine (TMR) fluorophore that is able to detect cocaine in aqueous environments.[65] In the absence of cocaine, the labeled aptamer adopts a conformation in which TMR interacts with the surrounding guanine nucleotides. As a consequence of these interactions, TMR suffers from restricted freedom, which is reflected in high fluorescence anisotropy (unequal intensities along different axes of polarization). However, upon binding of cocaine to the aptasensor there is a change in the conformation and also an alteration in the TMR–guanine interactions, which is reflected by a decrease in the fluorescence anisotropy (Figure 26). The best fluorescence anisotropy changes are obtained in the pH range of 7.0 to 8.5 at 10 °C. Moreover, the presented aptasensor allows the direct detection of cocaine with a limit of detection of 5 μM and also enables the detection of

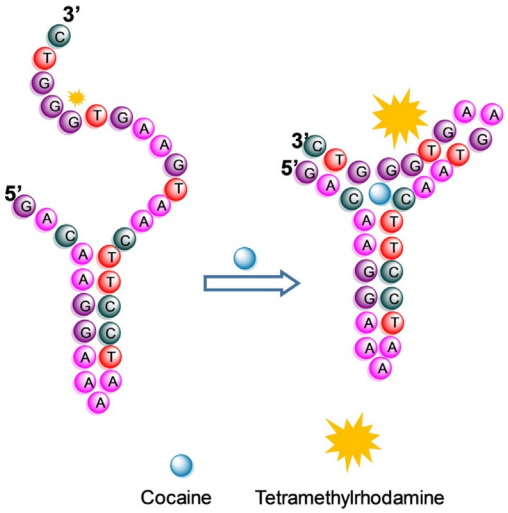

Figure 26. Schematic representation of the conformational change in the cocaine aptasensor that diminishes fluorescence emission of the TMR fluorophore attached to a G base in the presence of cocaine.

the drug spiked in diluted serum and urine samples. The system has also been tested against theophylline, caffeine, bovine serum albumin, immunoglobulin G, and a few amino acids, including arginine, phenylalanine, and aspartic acid. No remarkable fluorescence changes are observed, even at high concentrations.

Dong and co-workers delineate the development of a simple and easy to prepare colorimetric aptasensor for cocaine detection in aqueous solutions.[66] Double-stranded (ds) DNA can act as an efficient template for the formation of highly emissive copper nanoparticles (CuNPs) by using low concentrations of $CuSO_4$. However, the ssDNA template does not support the formation of CuNPs. The design consists of the use of two ssDNA sequences, one of them the cocaine aptamer and the other its complementary counterpart. Both sequences hybridize to form dsDNA, which acts as a template for the formation of fluorescent CuNPs in the presence of $CuSO_4$. However, in the presence of cocaine, the dsDNA dehybridizes due to the selective binding of the aptamer sequence with the drug, which precludes the formation of the emissive CuNPs (Figure 27). Other analgesic drugs (e.g. pethidine and methadone) and the complete hydrolysate form of cocaine (ecgonine) induce negligible responses. Besides, this aptasensor shows a good linear relationship in the presence of cocaine with a limit of detection of 0.1 mM.

Li's group outlines the development of a system for the detection of cocaine by employing a cocaine aptamer as a recognition site, graphene oxide (GO) as the fluorophore, and gold nanoparticles (AuNPs) as the quencher.[67] The cocaine aptamer is divided into two different fragments, C1 and C2, that are covalently immobilized onto GO and the AuNPs, respectively. In the presence of cocaine, aptamers C1 and C2 hybridize. This induces spatial proximity between the AuNPs and GO with subsequent emission quenching of the latter (Figure 28). With this simple aptasensor, the limit of detection for cocaine is 0.1 mM. The system works well in biological fluids such as plasma and serum. Moreover, the authors find that 0.1 mM cocaine leads to fluorescence quenching, whereas no effect is observed in the case of pethidine and methadone, even at concentrations as high as 50 mM (500 times the concentration of cocaine).

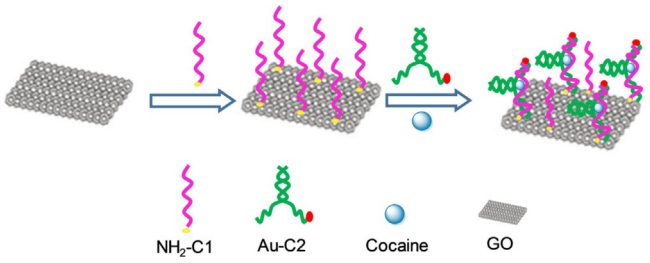

Figure 28. Schematic representation for cocaine detection through aptasensors based on graphene oxide and gold nanoparticles.

A similar GO-based aptasensor for cocaine detection by using cocaine-selective aptamers is also reported by Zhang and co-workers (Figure 29).[68]

Fan and co-workers present a bioassay strategy to detect cocaine on the basis of AuNPs and modified DNA aptamers.[69] In this design, the cocaine aptamer is divided into two pieces that present random-coil-like conformations (ACA-1 and ACA-

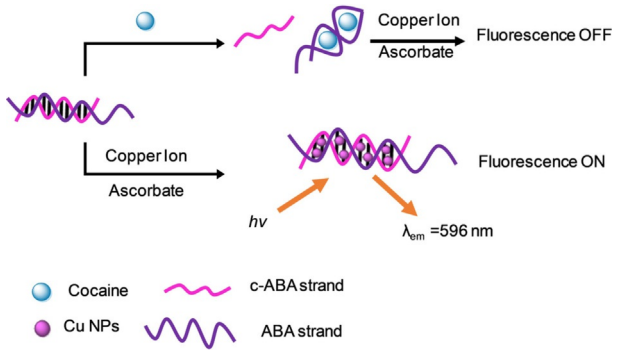

Figure 27. Schematic illustration for cocaine detection through aptamer conformational change.

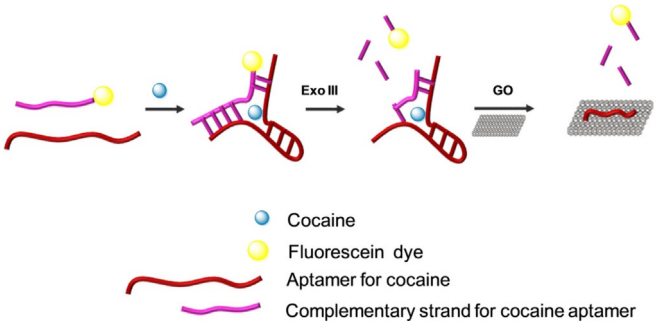

Figure 29. Schematic representation for the cocaine-sensing mechanism. In the presence of cocaine, the aptamer adopts a hairpin conformation and joins a complementary strand containing a fluorescein dye, which is released by enzyme Exo-III.

2). In the absence of cocaine, ACA-1 and ACA-2 spontaneously bind with the AuNPs, which stabilizes the AuNPs and precludes them from undergoing aggregation. Consequently, the typical plasmon band centered at $\lambda = 520$ nm and a dark red color are observed. However, in the presence of cocaine, the solution turns blue (absorption band at $\lambda = 650$ nm) due to the formation of a tertiary structure between ACA-1, ACA-2, and the drug, and this results in aggregation of the AuNPs (Figure 30). Using this strategy, cocaine in the low-micromolar range can be selectively detected by the naked eye. The limit of detection for cocaine is as low as 2 μM.

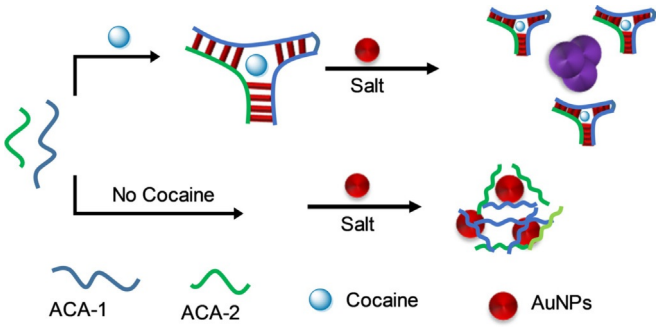

Figure 30. Cocaine detection by using aptamers ACA-1 and ACA-2. In the presence of cocaine, aptamers ACA-1 and ACA-2 adopt a coil-like conformation, allowing AuNP aggregation and a color change.

Liu and co-workers report a similar aptasensor for cocaine detection by using aptamers previously immobilized on the surface of AuNPs (Figure 31).[70]

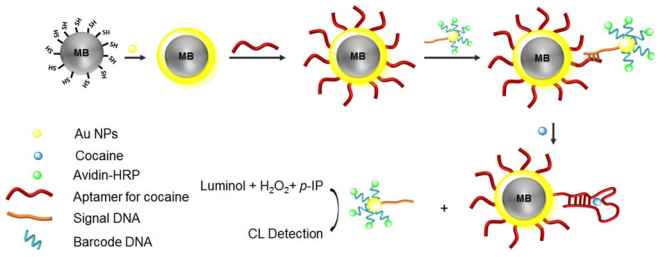

Figure 31. Cocaine aptamer anchored onto magnetic microbead surface. The aptamer changes its conformation in the presence of cocaine, releasing ssDNA and allowing chemiluminescence detection of the drug. HRP = horseradish peroxidase, *p*-1P = *p*-iodophenol, CL = chemiluminescence.

Zou and co-workers also use the combination of AuNPs and a triple-fragment aptamer for the selective optical detection of cocaine.[71] In the absence of cocaine, the three aptamer fragments interact with the AuNPs, which prevents their aggregation, and as a consequence, the solution remains red. In the presence of cocaine, the three aptamer fragments bind with the drug, leaving the AuNPs to form aggregates (Figure 32) with a color change to blue. The system is selective to cocaine, and no response is found in the presence of ecogonine methyl ester and benzoylecgonine. This aptasensor shows a gradual color change from red to blue as the concentration of cocaine

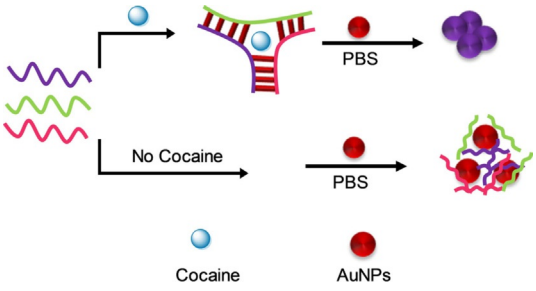

Figure 32. Three fragments of the cocaine aptamer are assembled in the presence of the drug, allowing AuNP aggregation and a color change.

is increased from 0 to 200 mM. A concentration of 100 mM cocaine in human urine or serum is readily detected by using this protocol.

Zhang and co-workers discuss a label-free fluorescence aptasensor for cocaine detection on the basis of the high affinity of a G-quadruplex for the ruthenium polypyridyl complex Ru[(bpy)$_2$(bqdppz)]$^{2+}$ (bpy = 2,2′-bipyridine, bqdppz = benzo[j]-quinoxalino[2,3-h]dipyrido[3,2-a:2′,3′-*c*]-phenazine).[72] The authors modify a cocaine-selective aptamer by extending the original sequence with guanine bases, which can form an intermolecular G-quadruplex under certain experimental conditions. The authors note that the Ru complex can be successfully embedded into the G-quadruplex structure to increase the fluorescence. However, in the presence of cocaine, the drug binds selectively to the aptamer, which results in dissociation of the G-quadruplex and release of Ru[(bpy)$_2$(bqdppz)]$^{2+}$ accompanied by significant emission quenching (Figure 33). The fluorescence intensity at $\lambda = 600$ nm decreases upon increasing the concentration of cocaine from 12 to 1300 nM, and the detection limit is as low as 5 nM. This system is highly selective towards cocaine over other small drugs such as caffeine, morphine, and theophylline. Furthermore, detection of cocaine in human serum can be performed with recoveries in the 94.5–103.6% range.

An example using modified aptamers grafted onto an optical fiber biosensing platform for the detection of cocaine is reported by He's group.[73] In this work, a cocaine aptamer is split into two fragments, and one of them is modified with a fluoro-

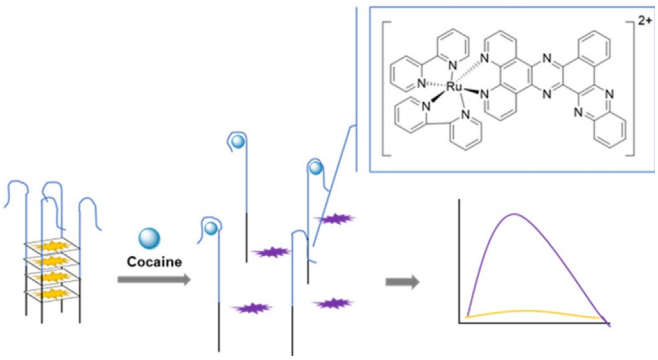

Figure 33. The intramolecular complex formed between the G-quadruplex and Ru[(bpy)$_2$(bqdppz)]$^{2+}$ is disassembled in the presence of cocaine, allowing its detection by emission quenching.

phore (Cy3) and the other with a quencher (BHQ = black hole quencher). In addition, the fluorophore-containing aptamer fragment is extended by 13 bases that can hybridize with an oligonucleotide previously immobilized on the optical fiber platform. In the presence of cocaine, the two fragments quickly form a three-way junction around the drug, which positions the fluorophore and the quencher in close proximity with subsequent emission quenching (Figure 34). At the same time, the tail of the three-way junction hybridizes with the oligonucleotide sequences immobilized on the optical fiber surface, and changes in the fluorescence are controlled by an evanescent wave. The aptasensor displays a highly competitive limit of detection of 165 nM and a sensing concentration range between 200 nM and 200 mM. The selectivity of this aptasensor has also been investigated against several compounds, including kanamycin, amikacin, and ibuprofen. No signal changes are observed, even at high concentrations (100 mM) of these compounds. This system can be used to detect cocaine in human serum.

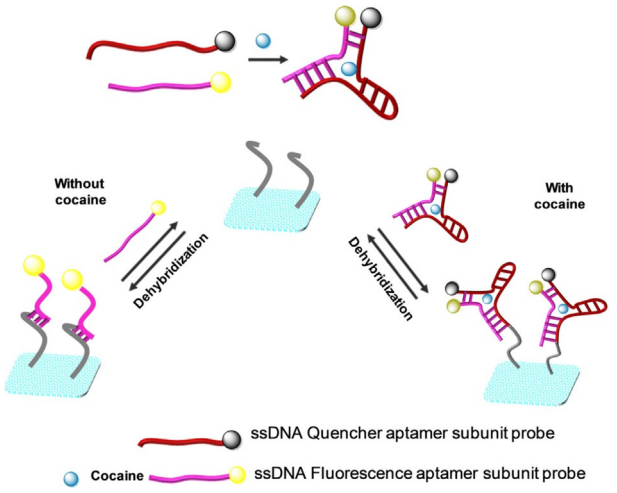

Figure 34. Schematic representation for cocaine detection through modified aptamers grafted onto an optical fiber biosensing platform.

Recently, Wang and co-workers have developed a new cocaine naked-eye detection method (Figure 35) by using paper microfluidic strips (PADs) coupled with gold nanoparticles and two cocaine aptamers (ACA-1 and ACA-2).[74] The PADs are fabricated by using a commercial wax printer to form three chambers (with different diameters) on the surface of chromatographic paper Whatmann No.1. More in detail, the chromatographic strip has, at the upper part, a chamber that contains 2 nmol AuNPs. In the middle chamber, ACA-1 and ACA-2 (0.6 nmol each) are placed. Finally, there is a chamber at the bottom of the strip for the samples. After adding the sample in the bottom chamber, the prepared test strip is placed in a carrier solution containing 2.8 M $MgCl_2$/50 mg mL^{-1} sucrose (300 μL). It is known that free aptamers can bind to the surface of AuNPs, preventing them from aggregating even in the presence of concentrated salts (red color). However, in the presence of cocaine, these aptamers bind to cocaine, leaving the

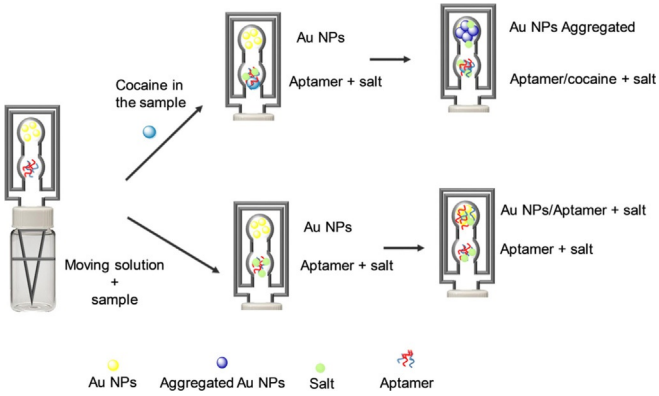

Figure 35. Schematic representation for cocaine detection by using AuNPs and aptamers.

AuNPs free to aggregate. The authors find that even at low concentrations of cocaine (10 μg) the carrier solution passes through the aptamer zone to the location of the AuNPs and the color changes from pink-red to gray in 5 min. In contrast, in the absence of cocaine, the moving solution arrives at the end of the strip and the AuNPs area remains red, which can be noted by the naked eye. The limit of detection for cocaine reported for this system is 2.5 μg. Besides, a high selectivity over other illicit drugs such as ephedrine, codeine, ketamine, amphetamine, morphine, and methamphetamine can be achieved. Furthermore, metabolites of cocaine, benzoylecgonine, and ecgonine methyl ester are unable to induce a color change.

Liu and Lu present a method for the detection of cocaine on the basis of the colorimetric change observed upon disassembly of AuNPs functionalized with different thiol-modified DNA sequences connected to a complementary DNA sequence (linker) and to the corresponding analyte aptamer.[75] In the absence of cocaine, gold nanoparticles form aggregates of thousands of nanoparticles (blue color due to an absorbance band centered at $\lambda = 700$ nm). However, in the presence of this drug, these nanoparticles separate from each other because of a conformational change in the aptamer upon binding to cocaine (Figure 36), and this changes the color of the solution to red (absorbance at $\lambda = 522$ nm). Characterization by transmis-

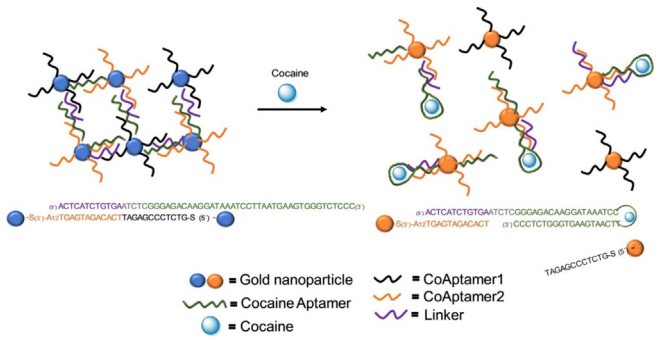

Figure 36. Cocaine detection through aptamer conformation changes in the presence of the drug.

sion electron microscopy after/before cocaine addiction confirms the disaggregation of the nanoparticles. Cocaine can be quantified in the range of 50 (LOD) to 500 μM within a 10 s period.

Liu et al. reported in 2016 a portable up-conversion nanoparticle (UCNP)-based paper device for cocaine detection.[76] The paper device is functionalized with polyethylenimine (PEI)-coated UCNPs and with the amine-modified ACA-1 fragment of the cocaine aptamer. Besides, another fragment of cocaine aptamer (ACA-2) bearing a thiol moiety is grafted onto the external surface of 16 nm AuNPs (Figure 37). In the presence of

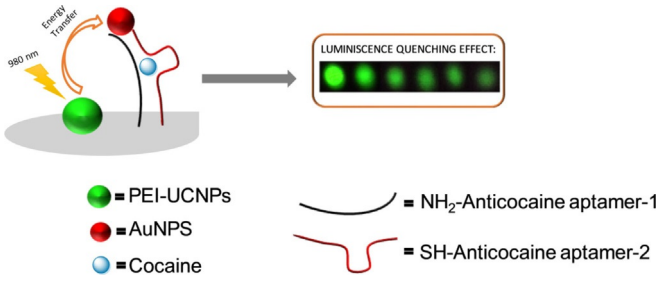

Figure 37. Luminescence quenching effect due to energy transfer between PEI-UCNPs and AuNPs if cocaine is present.

cocaine, both DNA fragments (ACA-1 and ACA-2) reassemble, and the luminescence of the UCNPs is quenched by the proximity of the AuNPs. This quenching effect can be attributed to the perfect match of the emission of the UCNPs and the absorption of the AuNPs and can be observed by the naked eye for qualitative analysis or recorded by a smartphone to convert data into RGB intensity for quantification. The limit of detection for cocaine is 10 nM, whereas in human saliva the minimum amount detected is 0.05 μM. Besides, recoveries in the 89–103 % range can be measured for cocaine-spiked samples of human saliva. On the other hand, neither ecgonine methyl ester nor benzoylecgonine induce any emission change.

Yu and co-workers report a cocaine detection method based on graphene oxide (GO) and on polymerase-aided isothermal circular strand-displacement amplification (ICSDA) combined with the use of the dye SYBR Green I (SGI).[77] The authors prepare a hairpin probe consisting of two different DNA fragments: 1) a cocaine aptamer; 2) a region designed to hybridize with a primer. In the absence of cocaine, the 3′-phosphorilated end of the hairpin probe oligonucleotide chain avoids polymerase elongation, whereas in the presence of the drug a conformational change exposes the 3′-single-stranded tail that hybridizes with the primer and allows initiation of the polymerase chain reaction. This process forms large amounts of dsDNA, with low affinity toward GO, which intercalates the SGI dye, and its fluorescence is observed. In addition, in the absence of cocaine, dsDNA is not formed, and the hairpin probe and SGI are adsorbed onto GO with subsequent quenching of the emission of the fluorophore (Figure 38). The limit of detection for cocaine is estimated to be 190 nM, and the linear range is from 0.2 to 100 μM. Weak fluorescence emission in the presence of adenosine, caffeine, theophylline, and morphine hydrochloride is observed. Finally, good linear correlation from 0.5 to 100 μM is achieved for cocaine-spiked real urine samples (20-fold dilution).

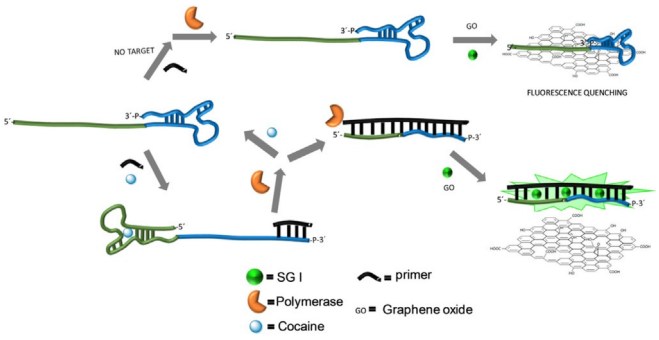

Figure 38. Representation of cocaine aptasensors combining GO, aptamers, and polymerase activity.

Yagci and co-workers assess a double fluorescence microwell assay that combines QDs labeled with cocaine antibodies with a polyphenylene-based polymer (PPP) containing β-cyclodextrins (CDs) derivatized with poly(ethylene glycol) (PEG) chains (Figure 39).[78] The PPP-CD-g-PEG polymer can be synthesized

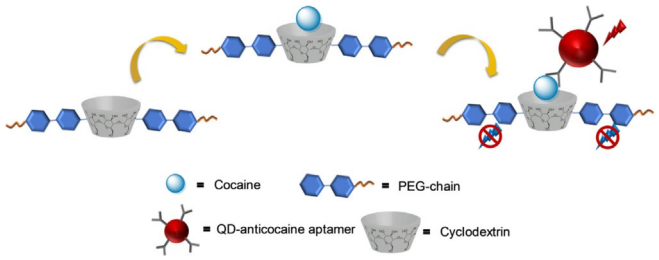

Figure 39. Schematic representation of the double fluorescence assay designed for the detection of cocaine.

by a Suzuki coupling reaction. In this polymer, the hydrophobic cavity of the CD is envisioned as a cocaine recognition site, whereas the PEG chains provide water solubility. The surface of the microwell is modified by grafting of the PPP-CD-g-PEG polymer. Cocaine forms inclusion complexes with the CD in the polymeric backbone. Then, the QDs are added, and they coordinate with cocaine through selective interaction of the drug with the antibodies that coat the nanoparticles. As a consequence, the emission of the QDs centered at $\lambda = 655$ nm ($\lambda_{ex} = 400$ nm) is enhanced. Besides, the intrinsic fluorescence emission of PPP-CD-g-PEG at $\lambda = 410$ nm ($\lambda_{ex} = 330$ nm) is quenched by the adsorbed QDs. By using this methodology, a linear range from 10 to 100 nM of cocaine with a limit of detection of 13.35 nM is obtained. Negligible response is obtained in the presence of methamphetamine, codeine, tetrahydrocannabinol, nicotine, cotinine, and benzoylecgonine. Finally, synthetic serum samples spiked with known cocaine amounts have been analyzed, and the results obtained have been compared to those obtained by using LC–MS/MS; good agreement is observed.

Hu et al. present a novel colorimetric cocaine biosensor based on Au@Ag core–shell nanoparticles (Figure 40).[79] For this purpose, Au@Ag nanoparticles are functionalized with a ssDNA reporter (RP), and then, magnetic beads (MBs) are prepared and coated with a capture ssDNA (CP). RP and CP are

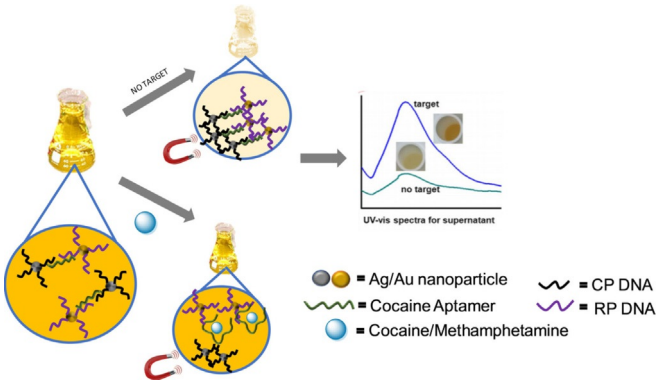

Figure 40. Schematic illustration of the mechanism for the detection system based on gold nanoparticles core–shell functionalized with aptamers.

designed to present complementarity with the cocaine aptamer. In the absence of cocaine and in a solution containing its aptamer, RP-functionalized Au@Ag nanoparticles and CP-coated MBs aggregate and can be removed upon application of an external magnetic field. However, if cocaine is present, its selective coordination with the aptamer inhibits nanoparticle aggregation, and the solution remains yellow (absorbance of the nanoparticles centered at $\lambda = 400$ nm). With this protocol, the limit of detection for cocaine is 0.5 nM with a linear response of 0.5 to 200 nM. The system does not respond to the presence of other illicit drugs such as ketamine, norketamine, morphine, cathinone, methacathinone, 3-trifluoromethyphenylpiperazine, and MDA. A similar biosensor can be prepared for sensing methamphetamine with a limit of detection of 0.1 nM.

Leung and co-workers describe a label-free switch-on luminescent sensor for the detection of cocaine.[80] The authors design two DNA oligomers composed of a fragment of the cocaine aptamer and a fragment able to form G-quadruplex structures. In the presence of both cocaine and an iridium complex, the two aptamer fragments came together to allow the formation of a G-quadruplex structure, which gives a luminescent response. The ability to form the G-quadruplex structure with different iridium complexes has been studied. The best response is observed with **45** (Figure 41), as the size and shape of the N^N ligand is crucial for construction of the G-quadruplex structure. The limit of detection of the aptasensor with complex **45** for cocaine is 30 nM. Besides, the aptasensor is selective for cocaine in the presence of adenosine triphosphate, adenosine, warfarin, and suramin. Moreover, the formation of the G-quadruplex structure with other planar molecules such as ochratoxin A, thiazole orange, protoporphyrin IX, crystal violet, thioflavin T, and adenosine triphosphate has been studied, and only a weak luminescence response is observed.

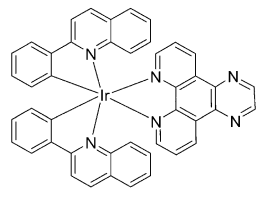

Figure 41. Chemical structure of iridium complex **45**.

Du et al. report a simple and sensitive DNAzyme-based colorimetric sensor for cocaine detection by using the 3,3,5,5-tetramethylbenzidine sulfate (TMB)/H_2O_2 reaction system.[81] For this purpose, the amino groups of functionalized magnetic nanoparticles (MNPs) are linked covalently to a thiolated cocaine aptamer fragment (C2). On the other hand, another cocaine aptamer fragment is extended with a G-enriched strand AG4 (C1-AG4). In the presence of cocaine, the C2 layer on the MNPs hybridizes partly with C1-AG4 to result in the folding of the aptamer into a three-way junction on the surface of the MNPs to form a MNPs-C2–cocaine–C1-AG4 complex. Using an external magnet, the nanoparticles can be separated from the solution (Figure 42). Then, the addition of hemin to the MNPs-

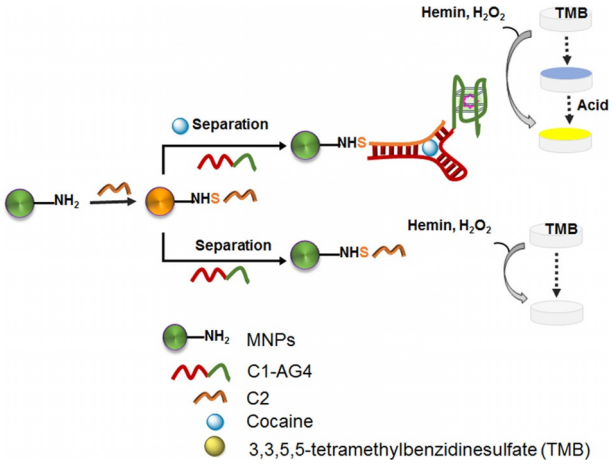

Figure 42. Colorimetric assay for cocaine detection by using aptamers, hemin, and TMB.

C2–cocaine–C1-AG4 complex promotes the formation of a DNAzyme, which catalyzes the TMB/H_2O_2 reaction system to yield a change in the color of the solution from colorless to yellow. In the absence of cocaine, the separated MNPs do not include C1-AG4; thus, no background signal can be produced. Using these aptasensors, drug concentrations of 100 nM can be directly detected by the naked eye, with a limit of detection of 50 nM. Besides, this protocol shows high selectivity for cocaine over ecgonine, pethidine, and methadone, which do not induce any color changes.

Silver nanoclusters (AgNCs) can be used as an indicator for cocaine detection in the presence of DNA templates utilizing the advantages of the nicking endonuclease-assisted signaling amplification (NEASA) strategy (Figure 43).[82] The reported aptasensor consists of three different DNA sequences, DNA1, DNA2, and DNA3. The first one is designed to contain three domains: the cocaine aptamer, a sequence that is complementary to DNA2, and a nicking endonuclease (Nb.BbvCI) enzyme recognition sequence. On the other hand, DNA2 includes two AgNCs template segments (coordinates with metallic AgNCs)

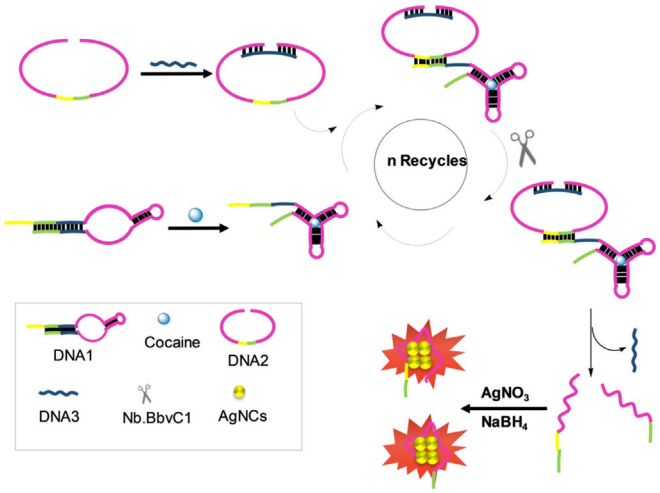

Figure 43. Schematic representation of fluorescent Ag nanocluster formation in the presence of cocaine.

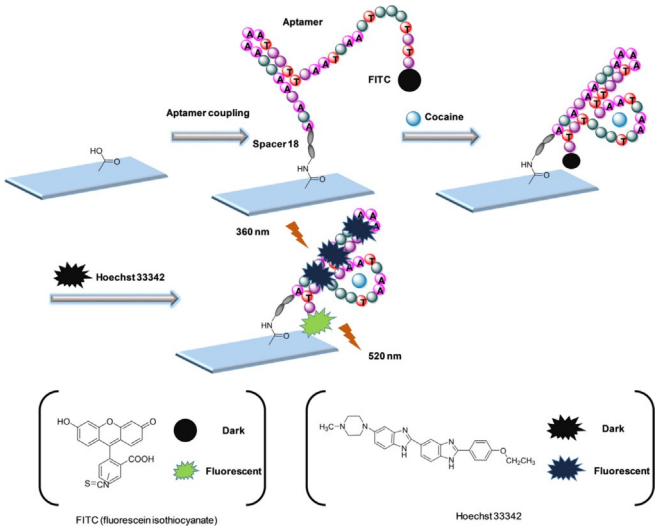

Figure 44. Scheme for cocaine detection by using aptamers grafted onto polydimethylsiloxane glass. In the presence of cocaine, the aptamer adopts a specific conformation that interacts with Hoechst 33342. This dye restores FITC emission.

and the recognition sequence and cleavage site for Nb.BbvCI. Finally, DNA3 is designed to be partly complementary to both ends of DNA2. It must be noted that the free AgNC template segments act as a scaffold for the synthesis of fluorescent silver nanoclusters in the presence of Ag^+ through its reduction with $NaBH_4$. Therefore, in the absence of cocaine, DNA3 and DNA2 undergo hybridization to form a closed circular structure that keeps the AgNC template segment in a rigid stage that cannot combine with Ag^+ to form the fluorescent silver nanoclusters. However, the addition of cocaine to the solution induces opening of the structure due to the binding of cocaine to its specific aptamer; thus, hybridization between the three DNAs to form a DNA1–DNA2–DNA3 complex is facilitated. Then, selective enzymatic cleavage of the DNA2–DNA3 duplex by Nb.BbvCI results in the release of free AgNC template segments, and this induces the synthesis of fluorescent silver nanoclusters. The aptasensor shows high selectivity for cocaine over other common interferences such as ecgonine and benzoylecgonine. The prepared aptasensor presents a linear range from 2 nM to 50 mM cocaine with a limit of detection as low as 2 nM. Besides, the probe is able to detect cocaine in human serum with very high recovery values of around 98 to 99.8%.

Zhou and co-workers outline the construction of a new optical aptasensor for cocaine detection.[83] The system is based on a fluorescein isothiocyanate (FITC)-labeled aptamer that produces a conformational change from a partial single-stranded DNA to a double-stranded T-junction in the presence of cocaine (Figure 44). This change facilitates a minor-based energy transfer (MBET) between the FITC-labeled 3′-end of the aptamer and Hoechst 33342 bound to the double-stranded T-junction, and this leads to fluorescence emission at $\lambda = 520$ nm ($\lambda_{ex} = 360$ nm). The authors test the response of the aptasensor with benzoylecgonine and ecgonine methyl ester. None of the selected interfering chemicals induce any emission change. Furthermore, the limit of detection for cocaine is 0.2 μM.

Taking into account the previously exposed works, several strategies have been used to develop chromo- and fluorogenic probes for stimulant drugs, namely: 1) the formation of fluorescent complexes; 2) antibody-based systems; 3) the use of nanoparticles; 4) derivatization reactions; 5) spectral fluorescent signatures; 6) aptamer-based methods.

The formation of fluorescent complexes is one of the most exploited strategies. Probes reported within this approach change or enhance the fluorescence emission almost instantaneously and are easy to handle; some of them have the ability to detect drugs in the vapor phase, which considerably increases their potential use as a detection method in realistic settings. Besides, some of them can be fixed over surfaces. However, some limits of detection are relatively high, and some of the reported examples work in organic solvents or in mixed aqueous solutions. Several examples have high potential for real applicability. For instance, sensing strips for the naked-eye detection of cocaine by using antibodies and associated to a mobile app for quantification of the drug have been described. Sensory systems based on porous nanoparticles loaded with dyes/fluorophores show signal amplification features and allow drug detection in the vapor phase. Chemical derivatization of drugs with the aim to confer fluorescence to the final molecules is another widely followed strategy. The used reactions are fast and reliable, and some of the protocols described also include the use of mobile technology. In spite of these positive facts, none of the described examples based on this approach can detect drugs in the vapor phase. Other approaches involve the use of spectral fluorescence signature (SFS) measurements and artificial neuron networks for data treatment. This approach presents some drawbacks, such as the need for learning and validation steps and its complicated translation into an in-field system measurement. Moreover, a large percentage of the published examples dealing with the detection of well-known abuse drugs (such as cocaine and methamphetamine) are based on the use of aptamers (alone or grafted onto organic/inorganic supports). The selectivity

achieved with the use of aptamers is very remarkable. Besides, several aptamer-based detection systems are coupled with DNA replication processes for signal amplification, allowing very low limits of detection in the nanomolar range. However, from a technological point of view, these aptamer-based sensors are usually more expensive and complex than others described above.

4. Hallucinogenic Drugs

Hallucinogenic drugs include cannabis, psilocybin, lysergic acid diethylamide (LSD), peyote, and dimethyltryptamine (DMT), among others.[84] Historically, some of these drugs have been used for religious rituals. They cause the consumer to see and hear inexistent and unreal things, which causes the consumers to feel out of control or disconnected from their body and environment. Specifically, some of their most prominent effects occur in the prefrontal cortex-an area involved in mood, cognition, and perception, as well as other important regions in regulating arousal and physiological responses to stress and panic. These drugs can be found in some plants and mushrooms or can be man made. LSD, psilocybin, and DMT produce their effects through interaction with serotonin (5-HT) receptors. Others, the most, affect the *N*-methyl-D-aspartate receptor (NDMA-receptor), the κ-opioid receptor (KOR), and the neurotransmitter acetylcholine.

Badout and Andre take advantage of the intrinsic fluorescent properties of lisergamide (commonly known as LSD) to develop a low-costing and portable device for its detection.[85] LSD presents a fluorescence band in the $\lambda = 400–530$ nm range, depending on the solvent and pH. The apparatus is constructed to allow the naked-eye detection of LSD by comparing the emission of an LSD solution with its corresponding blank solution upon excitation with a mercury lamp by using both neutral and 1 M NaOH alkali solution as the solvent. If LSD solutions in neutral water are submitted to the mercury lamp, a characteristic blue emission is observed. This occurs also with other hallucinogens such mescaline, 2,5-dimethoxy-4-methyl amphetamine (DOM), psilocin, psilocybin, bufotenin, ibogaine, and phencyclidine. However, if they are dissolved in 1 M NaOH aqueous solution, only with LSD is a change in fluorescence emission to green observed. The limit of detection for LSD samples dissolved in neutral water is 50 ng, whereas that for LSD samples in alkali media increases to 260 ng.

There is only one example reported in this section, and it is anticipated that new chromo- and fluorogenic probes for the detection of hallucinogenic drugs will be developed in the near future.

5. Opiods

Opioids drugs such as heroin, codeine, morphine, fentanyl, hydrocodone, oxycodone, buprenorphine, and methadone act through opioid receptors in the spinal cord and brain.[86] These compounds have been used for centuries to treat pain, cough, and diarrhea. Nowadays, medical use is to treat acute pain. Opioids act by binding to opioid receptors, which are found principally in the central and peripheral nervous system and the gastrointestinal tract. The concurrent use of opioids with other depressant drugs such as benzodiazepines increases the rates of adverse events and overdose.

Baheri and co-workers propose a colorimetric method for the selective detection of opioid-based drugs such as morphine, codeine, oxycodone, noroxycodone, thebaine, tramadol, and methadone in aqueous media on the basis of color changes produced by the aggregation of AuNPs in the presence of these analytes that act as molecular bridges between them (Figure 45).[87] The sensing systems comprise four citrate-coated AuNPs with different particle sizes (diameters of 13, 23, 32, and 43 nm); these different AuNPs present different aggregation behaviors with selected drugs, which results in a fingerprint pattern in the spectra that can be translated by algorithmic pattern recognition [principal component analysis (PCA) and hierarchical cluster analysis (HCA)] in an array for the classification, identification, and quantification of these analytes. For each opioid and particle size, the difference in absorbance (ΔA) with the blank is used as a response, and the effects of critical parameters, such as pH, ionic strength, time of interaction, and analyte concentration, are evaluated. After optimization, discrimination of seven opioids is possible, with limits of detection of about 5 μmol L^{-1} (except for noroxycodone), and experiments with several potential interfering substances show negligible responses. Finally, color-difference maps are obtained before/after exposure for each opioid by using representative RGB wavelengths ($\lambda = 730$, 685, and 600 nm), and they show good accuracy and reproducibility.

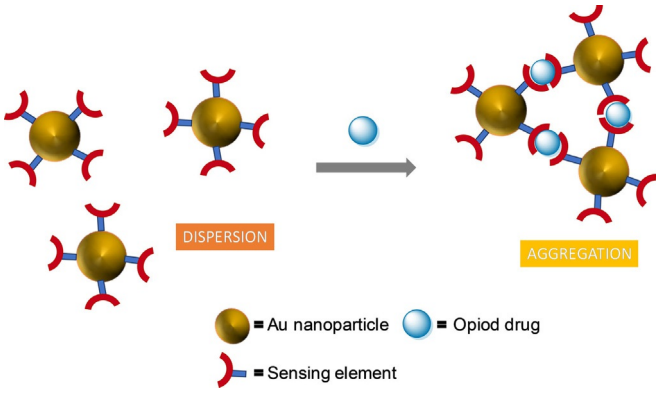

Figure 45. Schematic representation for the colorimetric detection of opioid drugs through AuNP color changes produced by nanoparticle aggregation.

Anzenbacher and co-workers present a new approach for sensing heroine, morphine, oxycodone, and their main metabolites on the basis of the interaction of these molecules with the flexible cavity of fluorescent acyclic cucurbituril (aCBs) derivatives (Figure 46).[88] Three aCBs functionalized with naphthalenes (with different degrees of steric hindrance) in the terminal walls are employed in the sensing protocol. The steric hindrance defines the diameter of the recognition cavity in the aCBs. The guests tested (i.e. heroine, morphine, oxycodone) share a common skeleton with small structural differences.

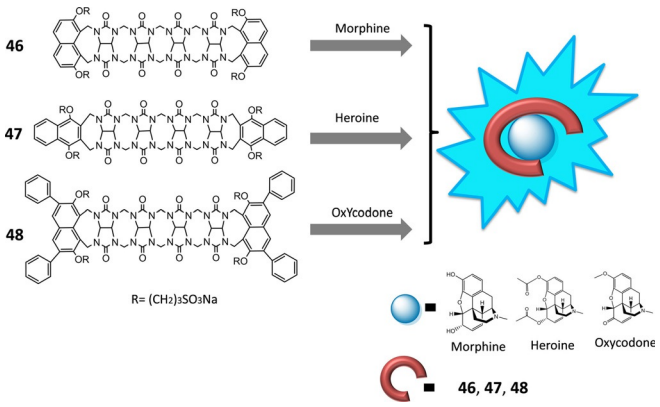

Figure 46. Fluorescence emission changes observed if morphine, heroine, and oxycodone interact with their corresponding cucurbituril (aCBs) derivatives.

Host–guest recognition results in fluorescence modification of the terminal naphthalene emission, and this induces a "turn-on" response for morphine and heroine as a consequence of the increased rigidity. However, in the case of oxycodone, and due to the quencher effect of cyclohexanone on naphthalenes, the fluorescence emission is diminished. Molecular dynamics calculations confirm that the naphthalene walls and the resultant cavity as well as guest uptake are decisive factors for fluorescence detection. The induced responses of these organic sensors with the studied opiates differ in the amplitude and saturation of the fluorescence change, in that the sensors all present different binding isotherms, and this suggests that they act as cross-reactive sensors. Furthermore, these organic probes show different behaviors for the studied parent drugs (i.e. morphine, heroin, and oxycodone) and their metabolites (i.e. normorphine, 6-monoacetylmorphine, morphine-3-glucuronide, morphine-6-glucuronide, noroxycodone, and oxymorphone), which makes it possible to determine both in a specific, qualitative, and quantitative manner. A qualitative assay has been performed in a high-throughput fashion by using linear discriminant analysis (LDA) for pattern recognition, and it shows three clusters consisting of the parent drugs and their corresponding metabolites. A general calibration makes it possible to detect the components of the clusters simultaneously with a single fluorescent reading. The limits of detection in aqueous media are 0.07 ppb for morphine and 82.5 and 2.78 ppb for the morphine metabolites morphine-3-glucuronide (M3G) and normorphine (Nmor), respectively. In human urine samples spiked with selected components, the limits of detection are 27.5, 972, and 71.3 ppb for morphine, M3G, and Nmor, respectively.

Only a few examples of chromo- and fluorogenic sensors for the detection of individual opioids have been described by now, and new examples in this area are expected to be reported in the future.

6. Conclusions

The problematic use of illicit drugs (both plant-based and synthetic derivatives) associated with their harmfulness to health and mortality has urged the scientific community to develop reliable methodologies to detect and quantify these lethal substances. We have herein reviewed probes for the chromo- and fluorogenic detection of illicit drugs. These probes (which can be simple molecules of more sophisticated systems involving biomolecules or hybrid organic–inorganic materials) provide excellent advantages over traditional analytical techniques, such as their chemical simplicity, ease of use, rapid response suitable for real-time on-site detection, and easy detection (in certain cases to the naked eye). However, in spite of these remarkable features, the development of chromo- and fluorogenic probes for the selective and sensitive detection of some illicit drugs is still poorly explored. In fact, more than half of the described chromo- and fluorogenic probes have been designed for the recognition/quantification of common plant-based drugs (such as cocaine), yet relatively few works describe the preparation of sensing systems for the detection of new synthetic illicit drugs. In addition, most chromo- and fluorogenic detection systems are designed for the detection of illicit drugs in solution, and there are very few examples for their detection in the vapor phase. Moreover, with the increasingly ubiquitous internet and other methods of communication, the presence of illicit drugs has expanded in recent years. As these synthetic drugs have not been approved for consumption or medical use, their long-term effects are potentially severe for humans. In this scenario, the development of new, rapid, inexpensive, and easy-to-use new probes for these new substances is of importance, and new advances in this field are expected in the near future.

Acknowledgements

We thank the Spanish Government [projects MAT2015-64139-C4-1-R and AGL2015-70235-C2-2-R (MINECO/FEDER)] and the Generalitat Valenciana (project PROMETEOII/2014/047) for support. S.E.S thanks the Ministerio de Economia y Competitividad for his Juan de la Cierva contract. B.L.T and E.G. thank the Spanish Government for their predoctoral grants. L.P. also thanks the Universitat Politècnica de València for his predoctoral grant.

Conflict of Interest

The authors declare no conflict of interest.

Keywords: chromophores · drugs · emission · fluorescent probes · sensors

[1] E. M. Komoroski, R. A. Komorsoki, J. L. Valentine, J. M. Pearce, G. L. Kearns, *J. Anal. Toxicol.* **2000**, *24*, 180–187.
[2] *Drugs of Abuse: A DEA Resource Guide*, U. S. Department of Justice Drug Enforcement Administration, **2017**.

[3] *World Drug Report*, United Nations Office on Drugs and Crime (UNODC), Inform **2017**.
[4] *European Drug Report: Trends and Developments*, European Monitoring Centre for Drugs and Drug Addiction (EMCDDA), Inform **2017**.
[5] A. Namera, A. Nakamoto, T. Saito, M. Nagao, *Forensic Toxicol.* **2011**, *29*, 1 – 24.
[6] a) A. Namera, M. Kawamura, A. Nakamoto, T. Saito, M. Nagao, *Forensic Toxicol.* **2015**, *33*, 175 – 194; b) D. A. Kidwell, J. C. Holland, S. Athanaselis, *J. Chromatogr. B* **1998**, *713*, 111 – 135; c) D. Cappelle, M. De Doncker, C. Gys, K. Krysuak, S. De Keukeleire, W. Maho, C. L. Crunelle, G. Dom, A. Covaci, A. L. N. van Nuijs, H. Neels, *Anal. Chim. Acta* **2017**, *960*, 101 – 109; d) R. A. Koster, J.-W. C. Alffenaar, B. Greijdanus, J. E. L. VanDerNagel, D. R. A. Uges, *Ther. Drug Monit.* **2014**, *36*, 234 – 243.
[7] Y. Li, U. Uddayasankar, B. He, P. Wang, L. Qin, *Anal. Chem.* **2017**, *89*, 8273 – 8281.
[8] V. de la Asunción-Nadal, S. Armenta, S. Garrigues, M. de la Guardia, *Talanta* **2017**, *167*, 344 – 351; b) R. Risoluti, S. Materazzi, *Talanta* **2016**, *153*, 407 – 413.
[9] C. Andreou, M. R. Hoonejani, M. R. Barmi, M. Moskovits, C. D. Meinhart, *ACS Nano* **2013**, *7*, 7157 – 7164.
[10] S. He, D. Liu, Z. Wang, K. Cai, X. Jiang, *Sci. China. Phys. Mech. Astron.* **2011**, *54*, 1757 – 1765.
[11] *Substance Abuse (Depressants or Sedative-Hypnotic Drugs)*, Harvard Health Publishing, Harvard Medical School, November **2014**.
[12] D. Zhai, B. K. Agrawalla, P. S. F. Eng, S. Lee, W. Xu, Y. Chang, *Chem. Commun.* **2013**, *49*, 6170 – 6172.
[13] U. S. Department of Justice Archive National Drug Intelligence Center (USDOJ), Usdoj.gov. 2012 – 2006 – 15, **2014**.
[14] D. Zhai, Y. Q. E. Tan, W. Xu, Y.-T. Chang, *Chem. Commun.* **2014**, *50*, 2904 – 2906.
[15] L. A. Baumes, M. B. Sogo, P. Montes-Navajas, A. Corma, H. Garcia, *Chem. Eur. J.* **2010**, *16*, 4489 – 4495.
[16] W. Wang, Z.-Z. Dong, G. Yang, C.-H. Leung, S. Lin, D.-L. Ma, *J. Mater. Chem. B* **2017**, *5*, 2739 – 2742.
[17] M. J. H. Al-Kaffiji, A. M. S. Al-Anbakey, *Int. J. Pharm. Pharm. Sci.* **2013**, *5*, 606 – 611.
[18] J. A. Morris, *J. Forensic Sci.* **2007**, *52*, 84 – 87.
[19] *Merck Manual Drug Information*, Provided by Lexi-Comp, last full review, May **2014**.
[20] A. Argente-García, N. Jornet-Martínez, R. Herráez-Hernández, P. Campíns-Falcó, *Sens. Actuators B* **2017**, *253*, 1137 – 1144.
[21] P. Campíns-Falcó, Y. Moliner-Martínez, R. Herráez-Hernández, C. Molins-Legua, J. Verdú-Andrés, N. Jornet-Martínez, Patent P201300436, **2013**.
[22] K. M. Elokely, M. A. Eldawy, M. A. Elkersh, T. F. El-Moselhy, *Curr. Chem. Res.* **2012**, *2*, 60 – 68.
[23] M. A. F. Elmosallamy, A. S. Amin, *Anal. Sci.* **2014**, *30*, 419 – 425.
[24] N. Mohseni, M. Bahram, *Anal. Methods* **2016**, *8*, 6739 – 6747.
[25] National Institute on Drug Abuse (NIDA), Misuse of Prescription Drugs, August **2016**.
[26] T. Sakai, N. Ohno, *Anal. Sci.* **1986**, *2*, 275 – 279.
[27] T. Sakai, N. Ohno, *Analyst* **1987**, *112*, 149 – 152.
[28] A. Argente-García, N. Jornet-Martínez, R. Herráez-Hernández, P. Campíns-Falcó, *Anal. Chim. Acta* **2016**, *943*, 123 – 130.
[29] E. Guler, T. Y. Sengel, Z. P. Gumus, M. Arslan, H. Coskunol, S. Timur, Y. Yagci, *Anal. Chem.* **2017**, *89*, 9629 – 9632.
[30] A. Chooduma, K. Parabuna, N. Klawacha, N. N. Daei, P. Kanatharana, W. Wongniramaikul, *Forensic Sci. Int.* **2014**, *235*, 8 – 13.
[31] A. Choodum, P. Kanatharana, W. Wongniramaikul, N. NicDaeid, *Sens. Actuators B* **2015**, *215*, 553 – 560.
[32] D. Moreno, B. Díaz de Greñu, B. García, S. Ibeas, T. Torroba, *Chem. Commun.* **2012**, *48*, 2994 – 2996.
[33] Y. Fu, L. Shi, D. Zhu, C. He, D. Wen, Q. He, H. Cao, J. Cheng, *Sens. Actuators B* **2013**, *180*, 2 – 7.
[34] M. He, H. Peng, G. Wang, X. Chang, R. Miao, W. Wang, Y. Fang, *Sens. Actuators B* **2016**, *227*, 255 – 262.
[35] B. Lozano-Torres, L. Pascual, A. Bernardos, M. D. Marcos, J. Jeppesen, Y. Salinas, R. Martínez-Máñez, F. Sancenón, *Chem. Commun.* **2017**, *53*, 3559 – 3562.
[36] C. He, Q. He, C. Deng, L. Shi, Y. Fu, H. Cao, J. Cheng, *Synth. Met.* **2011**, *161*, 293 – 297.
[37] D. Masseroni, E. Biavardi, D. Genovese, E. Rampazzo, L. Prodi, E. Dalcanale, *Chem. Commun.* **2015**, *51*, 12799 – 12802.
[38] F. Reviriego, P. Navarro, E. García-España, M. T. Albelda, J. C. Frías, A. Domènech, M. J. R. Yunta, R. Costa, E. Ortí, *Org. Lett.* **2008**, *10*, 5099 – 5102.
[39] H. Yamada, S. Ikeda-Wada, K. Oguri, *J. Health Sci.* **1999**, *45*, 303 – 308.
[40] K. Matsuda, T. Fukuzawa, Y. Ishii, H. Yamada, *Forensic Toxicol.* **2007**, *25*, 37 – 40.
[41] S. Rouhani, S. Haghgoo, *Sens. Actuators B* **2015**, *209*, 957 – 965.
[42] M. Maue, T. Schrader, *Angew. Chem. Int. Ed.* **2005**, *44*, 2265 – 2270; *Angew. Chem.* **2005**, *117*, 2305 – 2310.
[43] K. Basavaiah, J. Manjunathaswamy, *Turk. J. Chem.* **2002**, *26*, 551 – 558.
[44] A. D. Mosnaim, E. E. Inwang, *Anal. Biochem.* **1973**, *54*, 561 – 577.
[45] D. Wang, T. Liu, W. Zhang, W. T. Slaven IV, C. Li, *Chem. Commun.* **1998**, *1*, 1747 – 1748.
[46] A. M. El-Didamony, A. A. Gouda, *Luminescence* **2011**, *26*, 510 – 517.
[47] J. Mazina, V. Aleksejev, T. Ivkina, M. Kaljurand, L. Poryvkina, *J. Chemom.* **2012**, *26*, 442 – 455.
[48] K. Sefah, D. Shangguan, X. Xiong, M. B. O'Donoghue, W. Tan, *Nat. Protoc.* **2010**, *5*, 1169 – 1185.
[49] Q. Shi, Y. Shi, Y. Pan, Z. Yue, H. Zhang, C. Yi, *Microchim. Acta* **2015**, *182*, 505 – 511.
[50] K. Mao, Z. Yang, P. Du, Z. Xu, Z. Wang, X. Li, *RSC Adv.* **2016**, *6*, 62754 – 62759.
[51] B. Shlyahovsky, D. L. Y. Weizmann, R. Nowarski, M. Kotler, I. Willner, *J. Am. Chem. Soc.* **2007**, *129*, 3814 – 3815.
[52] F. Wang, L. Freage, R. Orbach, I. Willner, *Anal. Chem.* **2013**, *85*, 8196 – 8203.
[53] J. Wang, J. Song, X. Wang, S. Wu, Y. Zhao, P. Luo, C. Meng, *Talanta* **2016**, *161*, 437 – 442.
[54] J. Huang, Y. Chen, L. Yang, Z. Zhu, X. Yang, K. Wang, W. Tan, *Biosens. Bioelectron.* **2011**, *28*, 450 – 453.
[55] C.-Y. Zhang, L. W. Johnson, *Anal. Chem.* **2009**, *81*, 3051 – 3055.
[56] A. S. Emrani, N. M. Danesh, M. Ramezani, S. M. Taghdisi, K. Abnous, *Biosens. Bioelectron.* **2016**, *79*, 288 – 293.
[57] D. Roncancio, H. Yu, X. Xu, S. Wu, R. Liu, J. Debord, X. Lou, Y. Xiao, *Anal. Chem.* **2014**, *86*, 11100 – 11106.
[58] E. Guler, G. Bozokalfa, B. Demir, Z. Pinar-Gumus, B. Guler, E. Aldemir, S. Timur, H. Coskunol, *Drug Test. Anal.* **2017**, *9*, 578 – 587.
[59] A. Ribes, E. Xifré-Pérez, E. Aznar, F. Sancenón, T. Pardo, L. F. Marsal, R. Martínez-Máñez, *Sci. Rep.* **2016**, *6*, 38649 – 386458.
[60] L. F. Marsal, L. Vojkuvka, P. Formentin, J. Pallarés, J. Ferré-Borrull, *Opt. Mater.* **2009**, *31*, 860 – 864.
[61] M. Oroval, M. Coronado-Puchau, J. Langer, M. N. Sanz-Ortiz, A. Ribes, E. Aznar, C. Coll, M. D. Marcos, F. Sancenón, L. M. Liz-Marzán, R. Martínez-Máñez, *Chem. Eur. J.* **2016**, *22*, 13488 – 13495.
[62] M. N. Stojanovic, P. de Prada, D. W. Landry, *J. Am. Chem. Soc.* **2000**, *122*, 11547 – 11548.
[63] M. N. Stojanovic, P. De Prada, D. W. Landry, *J. Am. Chem. Soc.* **2001**, *123*, 4928 – 4931.
[64] M. N. Stojanovic, D. W. Landry, *J. Am. Chem. Soc.* **2002**, *124*, 9678 – 9679.
[65] Y. Liu, Q. Zhao, *Anal. Bioanal. Chem.* **2017**, *409*, 3993 – 4000.
[66] Z. Zhou, Y. Du, S. Dong, *Anal. Chem.* **2011**, *83*, 5122 – 5127.
[67] Y. Shi, H. Dai, Y. Sun, J. Hu, P. Ni, Z. Li, *Analyst* **2013**, *138*, 7152 – 7156.
[68] Y. Zhang, Z. Sun, L. Tang, H. Zhang, G.-J. Zhang, *Microchim. Acta* **2016**, *183*, 2791 – 2797.
[69] J. Zhang, L. H. Wang, D. Pan, S. P. Song, F. Y. C. Boey, H. Zhang, C. H. Fan, *Small* **2008**, *4*, 1196 – 1200.
[70] Y. Li, X. Ji, B. Liu, *Anal. Bioanal. Chem.* **2011**, *401*, 213 – 219.
[71] R. Zou, X. Lou, H. Ou, Y. Zhang, W. Wang, M. Yuan, M. Guan, Z. Luo, Y. Liu, *RSC Adv.* **2012**, *2*, 4636 – 4638.
[72] S. Zhang, L. Wang, M. Liu, Y. Qiu, M. Wang, X. Liu, G. Shen, R. Yu, *Anal. Methods* **2016**, *8*, 3740 – 3746.
[73] Y. Tang, F. Long, C. Gu, C. Wang, S. Han, M. He, *Anal. Chim. Acta* **2016**, *933*, 182 – 188.
[74] L. Wang, G. Musile, B. R. McCord, *Electrophoresis* **2018**, *39*, 470 – 475.
[75] J. Liu, Y. Lu, *Angew. Chem. Int. Ed.* **2006**, *45*, 90 – 94; *Angew. Chem.* **2006**, *118*, 96 – 100.
[76] M. He, Z. Li, Y. Ge, Z. Liu, *Anal. Chem.* **2016**, *88*, 1530 – 1534.
[77] L. Qiu, H. Zhou, W. Zhu, L. Qiu, J. Jiang, G. Shen, R. Yu, *New J. Chem.* **2013**, *37*, 3998 – 4003.

[78] M. Arslan, T. Y. Sengel, E. Guler, Z. P. Gumus, E. Aldemir, H. Akbulut, H. Coskunol, S. Timur, Y. Yagci, *Polym. Chem.* **2017**, *8*, 3333 – 3340.
[79] K. Mao, Z. Yang, J. Li, X. Zhou, X. Li, J. Hu, *Talanta* **2017**, *175*, 338 – 346.
[80] D.-L. Ma, M. Wang, B. He, C. Yang, W. Wang, C.-H. Leung, *ACS Appl. Mater. Interfaces* **2015**, *7*, 19060 – 19067.
[81] Y. Du, B. Li, S. Guo, Z. Zhou, M. Zhou, E. Wang, S. Dong, *Analyst* **2011**, *136*, 493 – 497.
[82] K. Zhang, K. Wang, X. Zhu, J. Zhang, L. Xu, B. Huang, M. Xie, *Chem. Commun.* **2014**, *50*, 180 – 182.
[83] J. Zhou, A. V. Ellis, H. Kobus, N. H. Voelcker, *Anal. Chim. Acta* **2012**, *719*, 76 – 81.
[84] *Drug Facts*, National Institute on Drug Abuse (NIDA), Hallucinogens, January **2016**.
[85] P. Baudot, J.-C. Andre, *J. Anal. Toxicol.* **1998**, *7*, 69 – 71.
[86] National Institute on Drug Abuse (NIDA), Misuse of Prescription Drugs, August **2016**.
[87] N. Mohseni, M. Bahram, T. Baheri, *Sens. Actuators B* **2017**, *250*, 509 – 517.
[88] E. G. Shcherbakova, B. Zhang, S. Gozem, T. Minami, P. Y. Zavalij, M. Pushina, L. D. Isaacs, P. Anzenbacher, *J. Am. Chem. Soc.* **2017**, *139*, 14954 – 14960.

Received: March 7, 2018

